

## Evaluating the Effectiveness of Various Blast Loading Descriptors as Occupant Injury Predictors for Underbody Blast Events

Kumar B Kulkarni  
ESI US Inc  
Troy, MI

Jaisankar Ramalingam, Ravi Thyagarajan  
US Army, TARDEC  
Warren, MI

### ABSTRACT

*It is of considerable interest to developers of military vehicles, in early phases of the concept design process as well as in Analysis of Alternatives (AoA), to quickly predict occupant injury risk due to under body blast loading. The most common occupant injuries in these extremely short duration events arise out of the very high vertical acceleration of vehicle due to its close proximity to hot high pressure gases from the blast. The primary objectives of this paper are to conduct an extensive parametric study in a systematic manner so as (1) to determine if a single blast loading parameter is sufficient to adequately characterize the occupant injury, at least for the duration of typical blast events (0-20ms) and (2) to create look-up tables and/or an automated software tool that decision-makers can use to quickly estimate the different injury responses for both stroking and non-stroking seat systems in terms of such a parameter.*

### INTRODUCTION

It is a well known fact that underbody blasts have become one of the most widespread reasons for warfighter casualties in recent wars [1-3]. Spinal injuries to occupants have particularly increased in theater from these roadside blast incidents, followed by tibia and lower leg injuries. To support the design and development of Mine-Resistant Ambush Protected (MRAP) military ground vehicles, mine blast underbody hull kits and mine blast seats, a suite of underbody modeling methods were quickly developed [4-11]. These modeling and simulation (M&S) methodologies are being continuously enhanced with ever-increasing capabilities to predict vehicle structural and occupant injury responses.

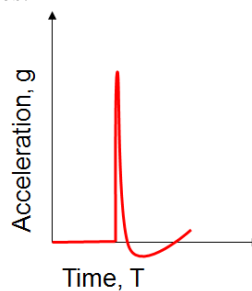


Fig 1: A typical blast pulse

It is of considerable interest to developers of military vehicles, in early phases of the concept design process, to quickly predict occupant injury risk due to under body blast loading [12]. The most common occupant injuries in these extremely short duration events arise out of the very high vertical acceleration of vehicle due to its close proximity to hot high pressure gases from the blast. A typical blast vertical acceleration history which is predominantly triangular shaped in nature is shown in Fig 1, and is often measured at a rigid location on the military vehicle to serve as a representative measure or a “signature” of the blast severity, and is

often referred to as the “blast pulse”. This can be thought of as being analogous to the crash pulse used in the automotive industry to serve as the loading that is experienced in the fore-aft direction by the structural components as well as the occupants in the vehicle interior. For example, the seats experience the pulse as a load at its structural attachment points. Other than the obvious difference in sign and direction (frontal crash results in vehicle deceleration in the fore-aft direction, while underbody blasts result in vehicle acceleration in the vertical direction), there are two other major differences between the blast pulse, and its frontal safety crash counterpart, namely:

- (1) the peak acceleration – the blast pulse tends to be 5-10 times *larger* in magnitude, and
- (2) the duration of the pulse – the blast pulse tends to be 3-5 times *shorter* than its crash counterpart.

As a common feature, both pulses serve as design criteria for development of seats, restraints and other safety features, and are even measured in a similar manner. The frontal crash pulse is usually the average fore-aft deceleration measured at one or more accelerometers at the stiff B-pillar/Rocker joint areas, while the blast pulse is usually the average vertical acceleration measured at one or more accelerometers at the stiff pillar/roof joint areas.

There has been a continual quest in the blast community of practice to define one or more loading parameters from the “blast pulse” that would by themselves, or in combination thereof, serve as indicators of blast severity and therefore occupant injuries, similar to the crash pulse scenario. For example, in automotive frontal crashes, the peak value in the crash deceleration pulse is one quantity that directly correlates to occupant injuries, everything else being constant. In the past, several similar loading parameters have been proposed for blast pulses, some examples of which are provided in the next section. Of these, the design community has mostly used change in velocity  $\Delta v$ , or to a much lesser extent, peak acceleration  $G_{peak}$ , to determine the severity of, and classify any given blast pulse.

The primary objectives of this paper are to conduct an extensive parametric study in a systematic manner so as (1) to determine if a single blast loading parameter is sufficient to adequately characterize the occupant injuries, at least for the duration of typical blast events (0-20ms) and (2) to create look-up tables or automated software tools that decision-makers can use to quickly estimate the different injury responses for both stroking and non-stroking seat systems in terms of such a parameter.

**BLAST LOAD INDICATORS/DESCRIPTORS**

In the past, several blast loading parameters have been proposed, alone or in combination, to serve as indicators or predictors of occupant injuries. Some examples of these are:

- 1) magnitude of the peak acceleration,  $G_{peak}$  in g’s,
- 2) time duration of pulse,  $T$  in milliseconds (ms),
- 3) rate of onset of acceleration,  $\dot{G}$  in g/ms,
- 4) change in velocity,  $\Delta v$  in m/s
- 5) effective-g (slope of the velocity profile)  $G_{eff}$  in g’s,
- 6) specific power,  $SP$  ( $G_{peak} * \Delta v$ ) in g-m/s, or  $m^2/s^3$ .

Of these, the Survivability design community has largely used change in velocity  $\Delta v$ , or to a lesser extent, peak acceleration  $G_{peak}$ , to describe the severity of, and classify any given blast pulse.

Fig 2 shows an example of a blast pulse with a peak acceleration of 200g and 10ms duration. The corresponding velocity profile is shown Fig 3.

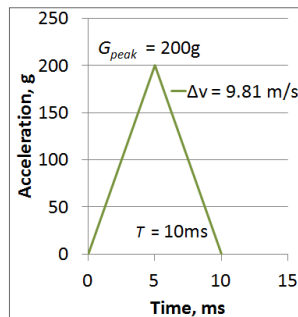


**Fig 2:** An example triangular blast pulse (Acceleration profile)

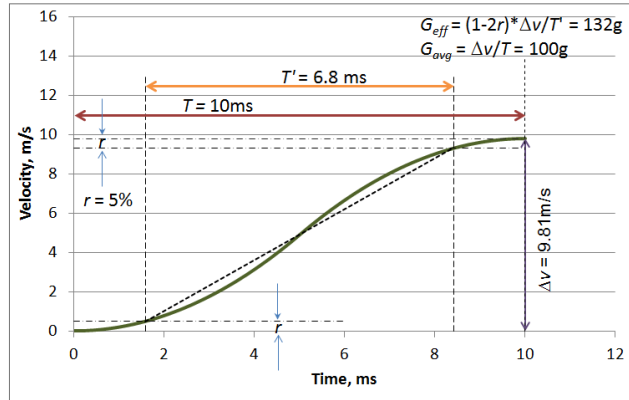


**Fig 3:** An example triangular blast pulse (velocity profile) Definition of effective-g is also shown

**G-Average**

G-average is simply defined as the slope of the velocity profile of any given blast pulse, i.e.,

$$G_{avg} = \Delta v / T$$

For a triangular pulse,  $G_{avg}$  is  $\Delta v / T = 1/2 * G_{peak}$

**Effective-g [13,15]**

Effective-g is defined [13] as the slope of the integral of the velocity trace; i.e.,

$$G_{eff} = \frac{1}{T} \int_0^T a dt = (V_f - V_0) / T = (\Delta v / T)$$

It has also been defined [15] as the steepest slope of the velocity profile which is found from the velocity trace by refining the value of  $\Delta v$  by ignoring the initial and final constant velocity “flat” regions (by a small factor  $r = 0.05$  or 5% of  $v$ ), as shown in Fig 3. For any value of  $r$ , effective-g for this pulse can be computed as  $(1 - r) * \Delta v / T$

An algebraic relationship can be derived defining the relationship between effective-g ( $G_{eff}$ ) and peak acceleration ( $G_{peak}$ ) for a triangular pulse as;

$$G_{eff} = G_{peak} \left( \frac{1 + \sqrt{2r}}{2} \right) \quad \text{for } (0 \leq r \leq 0.5)$$

For the rest of this paper, this second definition of  $G_{eff}$  is being adopted, though all observations made for any of the definitions is also applicable to the other since they are related by a simple factor  $(1 + \sqrt{2r})$ . It must also be mentioned here that any conclusions drawn with the choice of  $G_{avg}$  and/or  $G_{peak}$  as the blast loading parameter are also equally applicable to  $G_{eff}$  since all these quantities are related to each other by simple constants. For this reason, this paper may use these three quantities interchangeably, and without loss of generality.

For the limiting values of  $r = 0$  and  $r = 0.5$ , it can be readily seen that  $G_{eff}$  assumes the degenerated values of  $G_{avg}$  and  $G_{peak}$ , respectively.

**Specific Power [14]**

Specific power,  $SP$  is simply defined as  $SP = G_{peak} \cdot \Delta v$

For the example triangular pulse shown in Figure 3, the blast load descriptors defined above are as follows:

Delta-V,  $\Delta v = 9.81$  m/s

G-average,  $G_{avg} = \Delta v / T = 1/2 * G_{peak} = 100g = 981 \text{ m/s}^2$

Effective-g,  $G_{eff} = 132g$  (for  $r = 0.05$ ) =  $1295 \text{ m/s}^2$

Specific Power,  $SP = 19247 \text{ m}^2/\text{s}^3$

**BLAST SIMULATION MODEL**

Two setups of the dynamic simulation model of a vertical blast loading simulator are shown in Fig 4 and 5. In the first setup, a 50<sup>th</sup> percentile Humanetics’ Finite Element (FE)-based Hybrid-III Anthropomorphic Test Dummy (ATD) model (v7.1.6) in LSDYNA<sup>®</sup> format is seated on a rigid finite element seat with a five point seat belt as shown in Fig 4. This seat is rigidly placed on a vertically sliding platform (not shown in figure) where the blast pulse was input as base excitation. A typical run time for a FE-based simulation lasting 100ms duration is about two hours using 16 processors on an Intel x86-64 based Linux server.

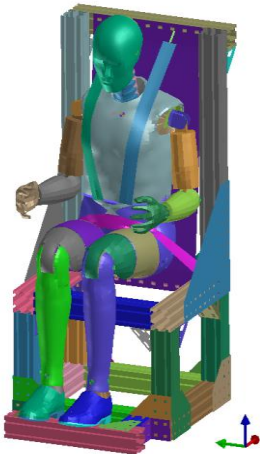


**Fig 4:** LSDYNA dynamic simulation model including Humanetics v7.1.6 Hybrid III 50th percentile ATD model

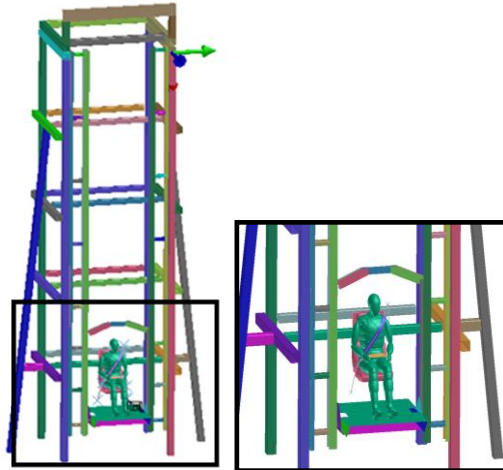


**Fig 5:** MADYMO dynamic simulation model including Q-version of Hybrid III 50th percentile ATD



**Fig 6:** Photograph of a typical drop tower test fixture

In the second setup, a vertical blast loading sled is constructed using finite elements of assigned rigid material. A MADYMO<sup>®</sup> rigid multibody (RMB)-based model of the 50<sup>th</sup> percentile Hybrid-III ATD (Q version) seated on a RMB seat, with a three point seat belt, is attached to a vertically sliding platform where the blast pulse was input as base excitation. A typical run time for a RMB-based simulation lasting 100ms duration is about 20 minutes using a single processor on an Intel x86-64 based Linux server.

A vertically sliding platform also known as a drop tower test fixture is shown in Fig 6. ATDs can be seated and the platform, including the seat and ATD, dropped from a suitable height to achieve any desired  $\Delta v$  over the duration  $T$ . The target pulse can be achieved by controlling the energy absorption characteristics of the floor on which the platform is dropped upon. Alternatively, a base excitation can be provided to the sliding platform in the upward vertical direction to achieve any given pulse if the fixture is so equipped (Also known as vertical sled). These two scenarios are completely equivalent in the occupant response behavior for the same given pulse.

Occupant injuries recorded from both these approaches were compared against those measured during physical tests. The resulting comparison showed no significant differences between the two approaches. Therefore the ensuing parametric modeling and simulation (M&S) study, involving a large number of simulations, was conducted on the latter multibody-based MADYMO<sup>®</sup> model since the run times for the latter are significantly lower than that of the FE-based model.

A parametric study was conducted by varying the peak acceleration from 10g -1200g, and duration of the pulse from 2.5ms to 60ms (a total of thirteen distinct duration levels) such that  $\Delta v$  is varied to a maximum value of about 15 m/s. The blast pulses with the minimum and maximum amplitudes from these thirteen duration levels are shown in Fig 7. In addition to a rigid seat without an energy-absorbing (EA) mine blast feature, two other generic EA blast mine seats of different ratings (EA1, EA2) were also used in the study (Fig 8). As may be observed from the figure, both EA seats have the same amount of stroke, but EA2 is softer in that it strokes at a lower limiting force level than EA1.

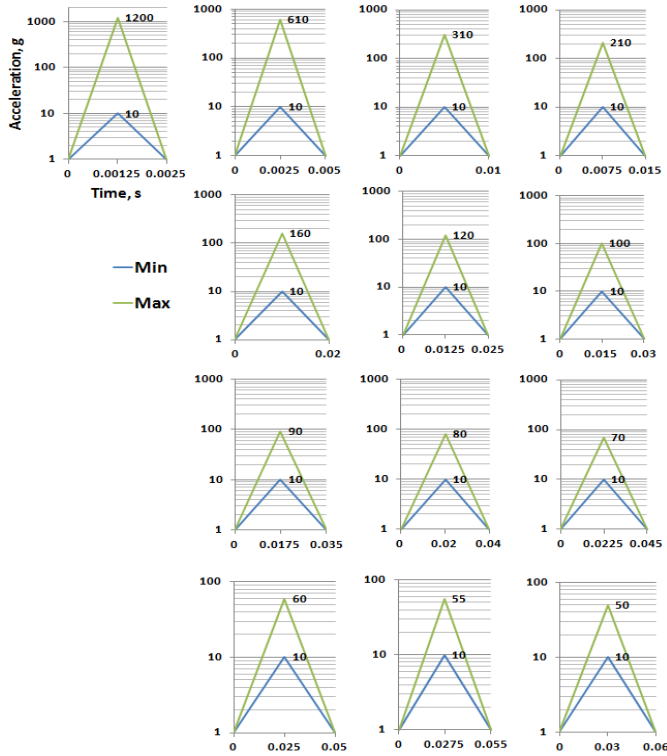


**Fig 7:** Blast pulses with minimum and maximum amplitude for the thirteen duration levels considered in this study.

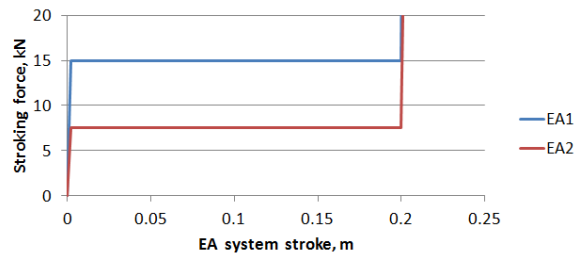


**Fig 8:** Two generic seat EA systems characteristics considered. Baseline EA (EA1) and Softer EA (EA2)

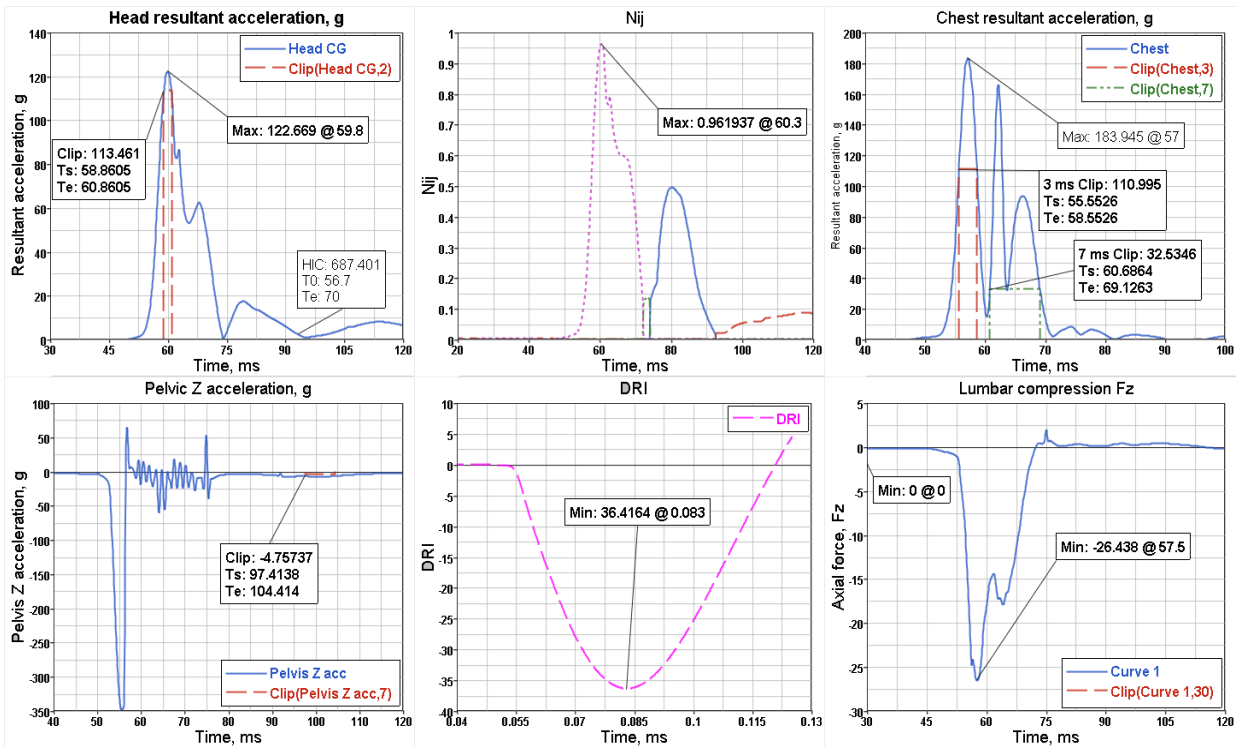


**Fig 9:** Recording occupant injury metrics

A total of ten different upper body injuries were recorded and monitored, namely:

- (1,2,3) Peak, 2ms clip and HIC<sub>15</sub> criterion of the head resultant acceleration,
- (4) N<sub>ij</sub> criterion for the neck injury,
- (5,6) 3ms and 7ms clips of chest resultant acceleration,
- (7) 7ms clip of pelvic vertical acceleration,
- (8,9) 7ms and 30ms clips of lumbar spine compression, and
- (10) Pelvic vertical Dynamic Response Index (DRI).

The sample size for each of the three seating variants consisted of 230 MADYMO<sup>®</sup> simulations, for a total of 690 data points. For each simulation, the ten occupant injuries are plotted and assessed using the post processing tool Hypergraph<sup>®</sup> as shown in Fig 9. In the next section, each of these ten injury responses are plotted against three leading blast loading indicators/descriptors, namely, Effective-g ( $G_{eff}$ ), Specific Power ( $SP$ ) and Delta-V ( $\Delta v$ ) to look for trends in the ability of the different descriptors to behave as predictors in a linear or quadratic sense, over the entire or limited ranges of pulse durations. For this purpose, linear and quadratic best fit analysis was also performed and overlaid against the data samples to evaluate how well the fits represented the underlying raw data.

**RESULTS/DISCUSSION**

**Parametric study**

Figs 10 and 11 are typical plots showing two occupant injuries, namely, Head Injury Criteria (HIC<sub>15</sub>) and the vertical Dynamic Response Index (DRI<sub>z</sub> or DRI), plotted against the three blast loading parameters. The first column of plots in Fig 10 are for the HIC<sub>15</sub> injury for the rigid seat, plotted against  $G_{eff}$ ,  $SP$  and  $\Delta v$ , from the top to the bottom, in that order. The second and third columns of plots are the same injury for the seats EA1 and EA2, respectively.

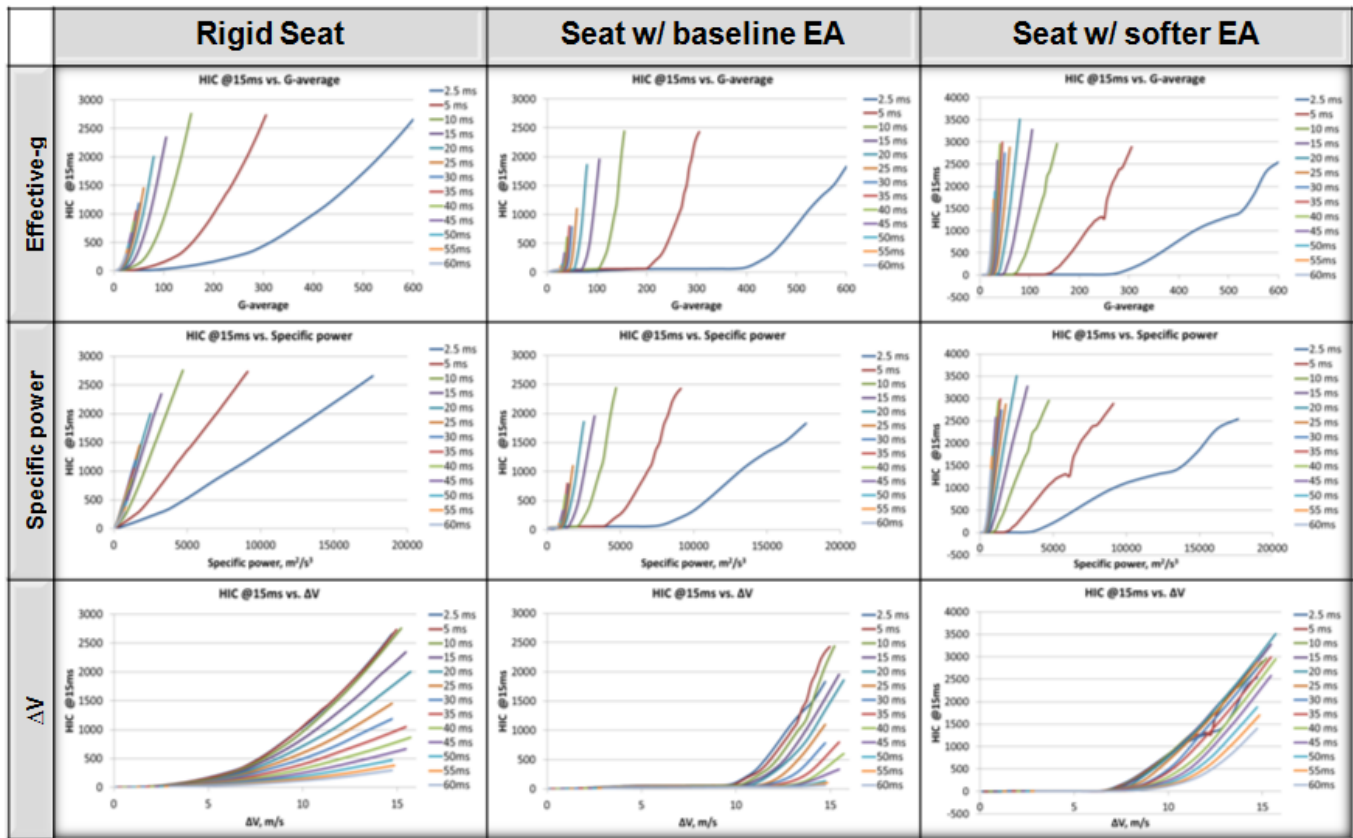


**Fig 10:** HIC<sub>15ms</sub> vs. blast loading parameters for three different seat types

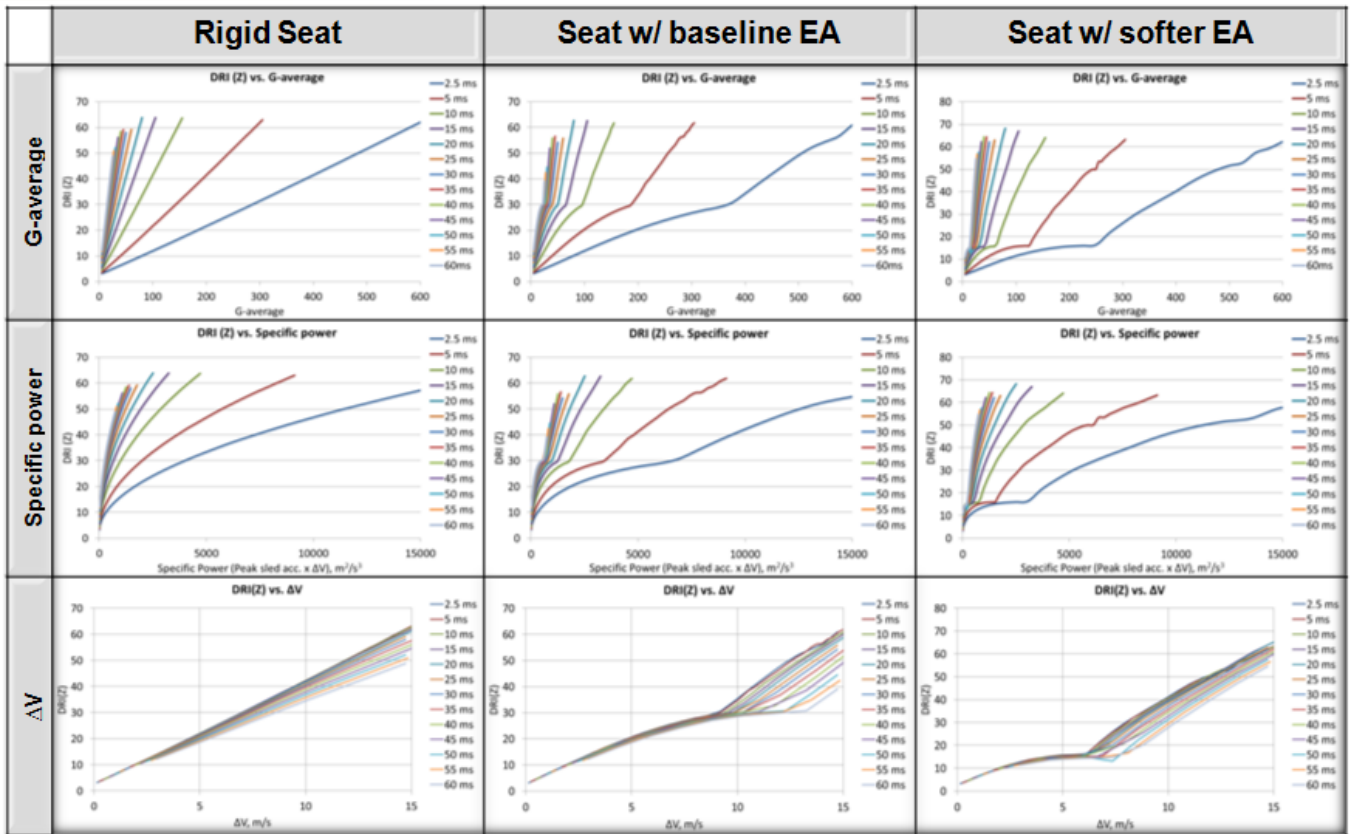


**Fig 11:** DRI vs. blast loading parameters for three different seat types

In each of the 9 plots in Fig 10, several curves can be seen. Each of these curves corresponds to a constant value of  $T$ , the duration of the blast pulse. In essence, they are nothing but iso- $T$  curves. Fig 11 is similar to Fig 10 except that it is for the DRI injury. Appendix A10-1 through A10-8 shows the corresponding data for the other eight occupant injuries. It may be observed from the figures that the injury responses are much more bunched together when plotted against  $\Delta v$ , as opposed to the other two blast loading parameters, thereby indicating a higher potential for  $\Delta v$  to be the single indicator being pursued. This trend to bunch together is even more pronounced in smaller intervals of  $T$ , that is, in 10 ms groupings such as 0-10, 10-20, 20-30, etc. It must also be mentioned here that the iso- $T$  curves, for all three load descriptors, tend to bunch together much better for larger values of pulse duration  $T$  ( $>30$  ms), but these durations are not typical of underbody blasts but more representative of standard automotive crash events.

To confirm the above in a quantitative manner, after the grouping was done in smaller sub-intervals of  $T$ , the time duration of pulses, linear and quadratic fit trend lines are drawn as shown in Figs 12 and 13 for  $HIC_{15}$  and DRI, respectively. Without loss of generality, only the iso- $T$  curves for 0-10 ms are shown for the injuries plotted against  $G_{eff}$  and  $SP$ , while iso- $T$  curves for 0-20 ms are shown for the injuries plotted against  $\Delta v$ . As can be clearly seen, the scatter in the data when plotted against  $G_{eff}$  and  $SP$  is so wide, no good fits are possible. In contrast, the same data when plotted against  $\Delta v$  yields closely bunched behavior, and good linear or quadratic fits to the same.

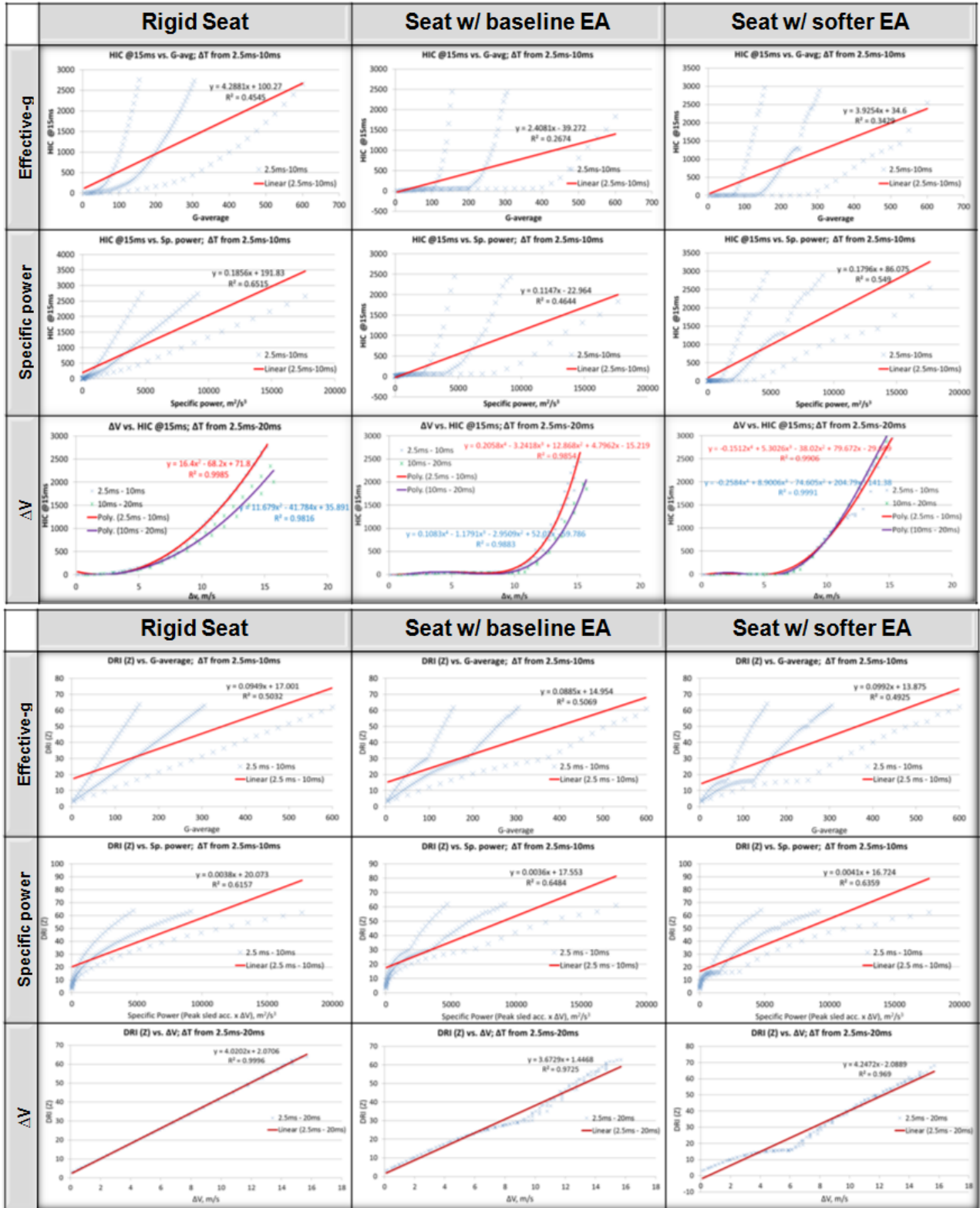


Fig 12 & 13: HIC<sub>15ms</sub> (Top) and DRI (Bottom) trends vs. blast loading parameters for three different seat types



Next, Correlation coefficients,  $r_c$  are computed for each of the ten injury parameters against the three blast loading indicators, and tabulated in Appendix Tables A1-A3, where,

$$r_c = \frac{\sum(x-\bar{x})(y-\bar{y})}{\sqrt{\sum(x-\bar{x})^2 \sum(y-\bar{y})^2}}$$

$x$  and  $y$  being the occupant injury parameter and blast injury indicator respectively. The value of  $r_c$  is such that  $-1 \leq r_c \leq +1$ . The + and - signs are used for positive and negative linear correlations respectively. A correlation coefficient  $>0.8$  is generally considered strong, whereas a correlation coefficient  $<0.5$  is considered weak. For each blast load indicator/descriptor, three columns are presented in Tables A1-A3 for each of the three seat configurations, namely, rigid, EA1 and EA2 considered in this study. It was determined that the probability of achieving a correlation coefficient,  $r_c > 0.8$  for pulse durations less than 10 ms, was highest at 77% for  $\Delta v$ , as compared to less than 20% for the other two indicators as shown in Table 1.

**Table 1:** Probability of achieving correlation coefficients of  $> 0.8$

| Probability of achieving $r_c > 0.8$ |         |            |           |
|--------------------------------------|---------|------------|-----------|
|                                      | 0-10 ms | 10 - 20 ms | 20 - 60ms |
| $G_{Eff}$                            | 0.00    | 0.80       | 0.60      |
| Sp. Pwr                              | 0.20    | 0.83       | 0.77      |
| $\Delta v$                           | 0.77    | 0.83       | 0.63      |

For pulse duration greater than 10ms and less than 20ms, all the three blast loading descriptors show a greater than 80% probability of achieving correlation coefficients of higher than 0.8. From these analyses, it can be concluded that  $\Delta v$  by itself is the best single indicator of injuries in the typical blast loading range of 0-20ms, independent of the seat type. It may be noted here that the low correlations are for noisy responses of lumbar compression (Table A10-6) and pelvic accelerations (Table A10-8) result in poor clip-based injuries.

The implication of the high values of  $r_c$  for the linear/quadratic fits to the injury data against the  $\Delta v$  load descriptor is that these fits can be used to predict injuries in the typical 0-20 ms loading durations, simply as a function of the single variable  $\Delta v$ , *without any dependence on the loading duration T*, or for that matter, any other variable. Conversely, the low fit values of  $r_c$  for Effective-G and Specific Power in the 0-10 ms loading duration regime is a clear indication that those loading parameters are poor candidates for being the single metric that can predict occupant injuries.

**Comparison against physical test data**

Injury data from different physical drop tower and vertical blast sled tests conducted with varying  $\Delta v$  were also gathered and plotted against corresponding data from the parametric M&S study. The physical test data, collected over 13 different tests performed at different times encompassing data with  $\Delta v$  variations from 2.3 to 6.9 m/s, and the duration  $T$  from 4 to 11 ms.

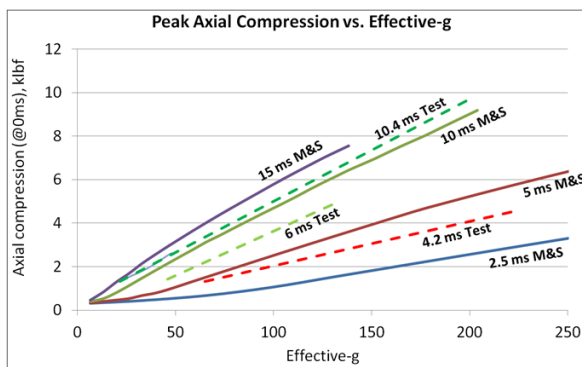


**Fig 14a:** Comparison of physical test data with M&S. Note injury dependence on  $T$

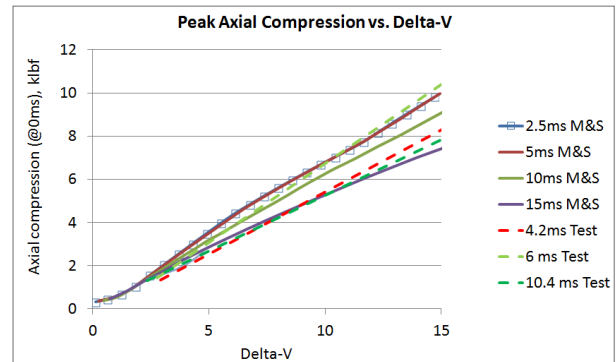


**Fig 14b:** Comparison of physical test data with M&S. Note injury dependence on  $T$  to a lesser degree

Figure 14a shows peak lumbar compression from physical tests overlaid against those from the parametric study, with  $G_{eff}$  as the loading parameter along the horizontal axis. Figure 14b is the exact same injury peak lumbar compression data plotted against  $\Delta v$  as the loading parameter along the horizontal axis. The following observations may be made from these two figures:

- (1) From Fig 14a, it may be seen that peak lumbar compression (from either physical tests or M&S) does not show any clear relationship with Effective-g, and that there is also a strong dependence on the duration of the pulse,  $T$ , as well.
- (2) However from Fig 14b, the same injury data (from both physical tests and M&S) show a marked linear relationship when displayed against  $\Delta v$  as the blast load indicator.
- (3) The trends in the results from modeling and simulation (M&S) closely agreed with those from physical tests, lending further credence to the findings of the parametric study.
- (4) The test data confirms the choice of  $\Delta v$  as the best single indicator of occupant injuries during typical blast event durations.

**Case Study 1 (Pulses with same  $\Delta v$ )**

In Ref [13], a study was performed with three different pulses of a constant  $\Delta v$  of 4.9 m/s and duration of 20, 40 and 80 ms, respectively. Figs 15 and 16 show these triangular pulses in acceleration and velocity domains respectively. Effective-g for these three pulses are 26.6, 13.3 and 6.65g.

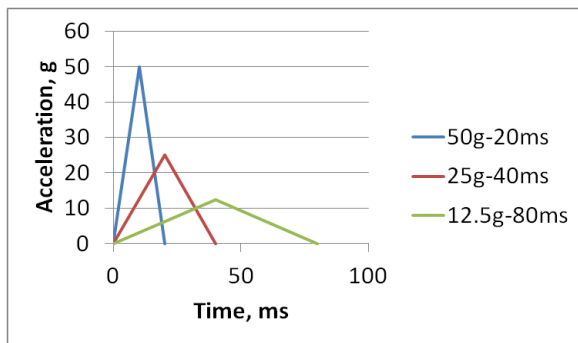


Fig 15: Three pulses all having  $\Delta v$  of 4.9m/s[13]

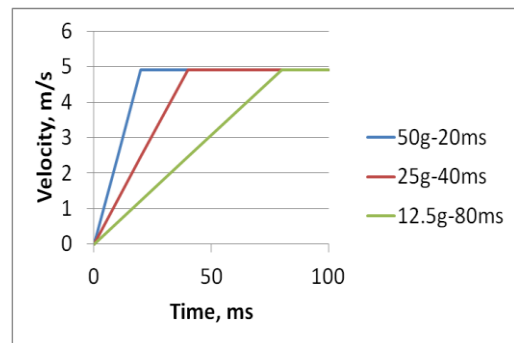


Fig 16: Three pulses all having  $\Delta v$  of 4.9m/s[13]

It was correctly pointed out that even though these pulses had the same  $\Delta v$ , the lumbar and DRI injuries were not the same, but in fact, demonstrated a somewhat linear relationship against  $G_{eff}$ . The implication of those findings was that  $\Delta v$  was not a good indicator of occupant injuries, because even when it was held constant, the injuries were varying. This section re-examines those findings in the context of the larger parametric M&S study described above.

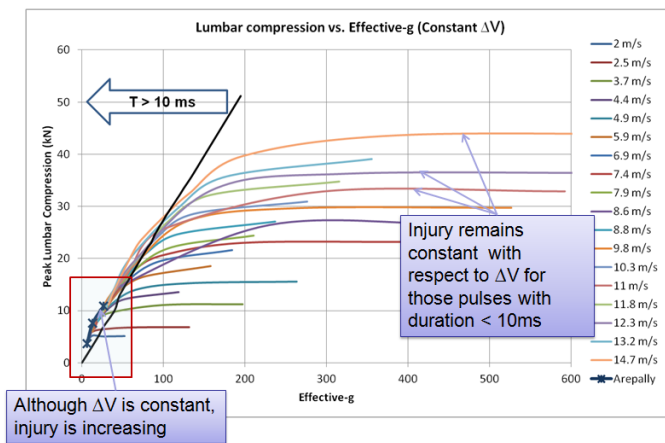


Fig 17: Constant  $\Delta v$ ; injury dependence on  $T$  ( $T > 10$ ms)

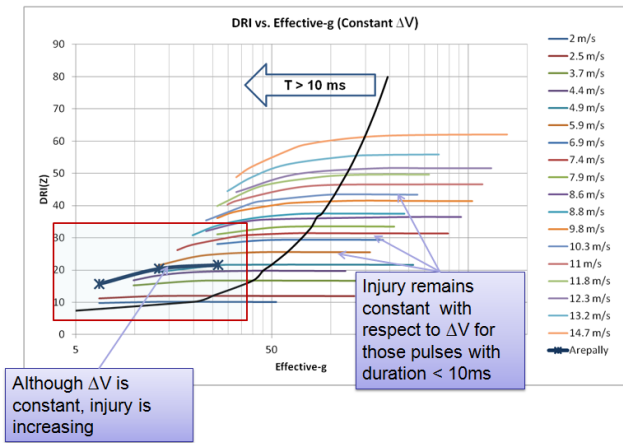


Fig 18: Constant  $\Delta v$ ; injury dependence on  $T$  ( $T > 10$ ms)

Figs. 17 and 18 show lumbar spine compression and DRI when subjected to these three pulse loadings, overlaid (using symbol X) against the data from the full parametric study. The data has been displayed as iso- $\Delta v$  lines here. The following observations may be made from these two figures:

- (1) The plots can be divided into two regimes, for  $T > 10$  ms, and  $T < 10$  ms with the dark line serving as the boundary.
- (2) In the regime to the left of the  $T=10$  boundary (i.e.,  $T > 10$ ), it can be seen that although  $\Delta v$  is constant, the occupant injuries are not constant but increasing against  $G_{eff}$ . In this region, it is indeed true that for a large variation in pulse durations (in this case 20-80 ms),  $\Delta v$  is not the best predictor of occupant injuries by itself,  $T$  also needs to be included. As mentioned before, in smaller subgroups 20-30, 30-40, etc.,  $\Delta v$  can still be used as a single variable to adequately predict the injuries, but not for the entire large interval in one shot.
- (3) For durations that are more typical of blast loading, the regime to the right of the boundary is applicable. It may be observed in this region that the injury curves tend to flatten out and the injuries indeed are constant at the same  $\Delta v$ .
- (4) On the other hand, it can be seen that because the injury curves are flattening out, pulses of different  $G_{eff}$  are giving rise to the same injury. That is, while the Injury- $G_{eff}$  relationship was linear for the choice of the 3 pulses chosen in Ref [13], that is not always necessarily the case.

**Case Study 2 (Pulses with same Effective-g)**

A contrarian study to Case Study 1 is now discussed. Three different pulses are chosen such that the peak acceleration is 200g for all three, and the duration of these pulses are 2.5, 5 and 10ms, respectively, resulting in an effective-g of 132g for all of them (Fig 19).  $\Delta v$  for these pulses are equal to 2.45, 4.9 and 9.81 m/s respectively. Figs 20 and 21 show the lumbar compression and DRI injuries when subjected to these pulse loadings. Fig 22 shows lumbar spine compression obtained from these three simulations overlaid (using symbol X) against the data from the full parametric study. The data in Figure 22 has been displayed as iso- $T$  lines. The following observations may be made from these two figures:

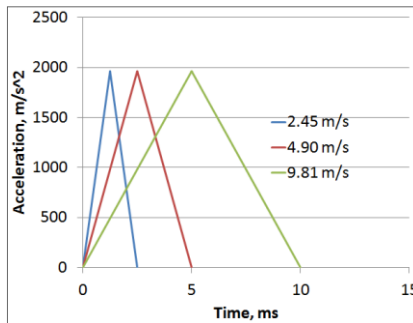


Fig 19: Three pulses all having an effective-g of 132g

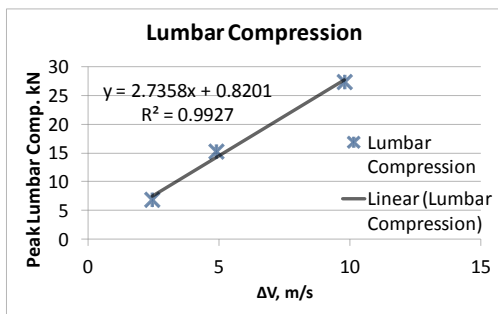


Fig 20: Same effective-g; increasing injury; exhibiting linear dependence on  $\Delta v$

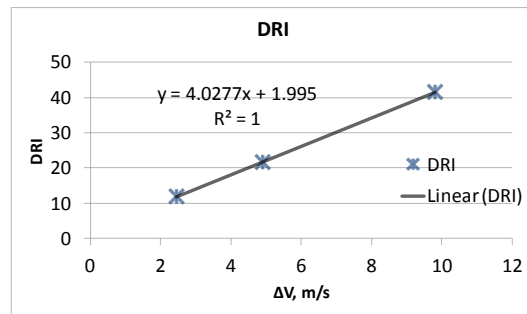


Fig 21: Same effective-g; increasing injury; exhibiting linear dependence on  $\Delta v$

- (1) Figs 20 and 21 show that the resulting injuries exhibit a good linear relationship with  $\Delta v$ .

- (2) Again, it can be noted how the iso- $T$  lines in Fig 22a are so bunched together, they can easily be represented by one line, thereby indicating very little dependence on  $T$  within the range of  $T$  under question (2.5-10 ms).
- (3) From Fig 22b, it can be observed that although effective-g is the same for the three cases, the resulting occupant injuries are not the same at all. In effect, this is similar to the pulses considered in Case Study 1 where three pulses with same  $\Delta v$  resulted in different injuries. Here, three pulses with the same  $G_{eff}$  result in different injuries.
- (4) Fig 22b also shows that effective-g by itself is not a good blast loading indicator when the pulse duration  $T$  is close to typical blast loading events of  $T < 20$ ms, since there is also a clear dependence of the injuries on  $T$ .

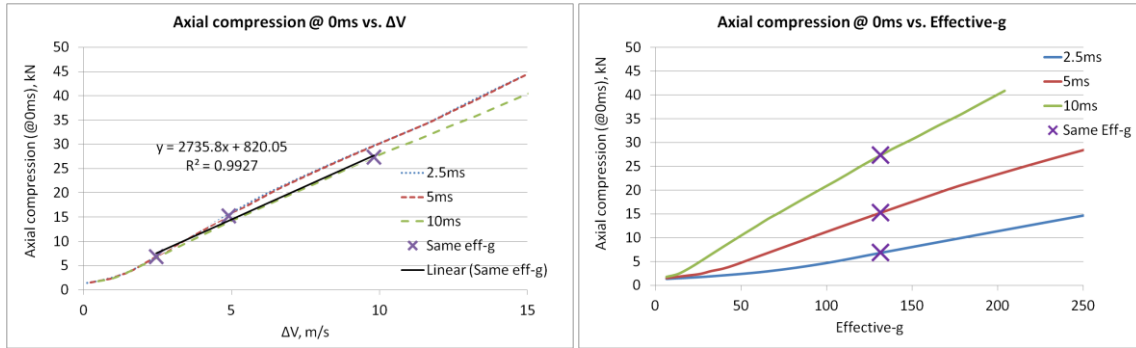


Fig 22 a & b: Injury exhibiting linear dependence on  $\Delta v$ ; same effective-g but increasing injury

**Metamodel**

Using the injury data obtained from the parametric M&S study, a metamodel was constructed using LSOPT<sup>®</sup>. Three-dimensional injury response surfaces were obtained for the ten injury parameters considered in this study from the LSOPT<sup>®</sup> simulations. Each of the injury surfaces was created as a function of the blast loading descriptor and the loading duration  $T$ . For example, Fig 23a shows contours of the peak lumbar compression response surface as a function of  $\Delta v$  and  $T$ , while Fig 23b shows contours of the same surface as a function of  $G_{eff}$  and  $T$ . Similar surfaces were also constructed for other injury parameters and they can be used as injury lookup tables with the blast loading descriptor and  $T$  as independent variables. The peak head acceleration injury response surface is shown in three dimensions plotted against  $\Delta v$  and  $T$  (Fig 24a) and against  $G_{eff}$  and  $T$  (Fig 24b). One important observation that may be made is that while both surfaces are mathematically equivalent, the uniformity of the surface against  $\Delta v$  makes it a more suitable candidate for reduced errors during the numerical interpolations required for injury predictions using the response surface.

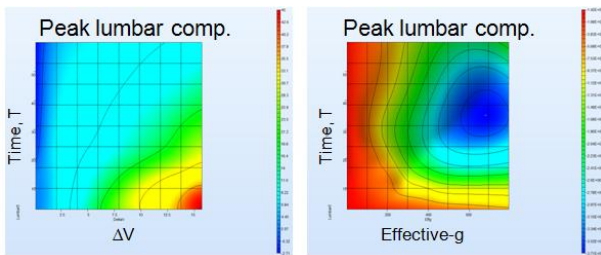


Fig 23 a & b: An example injury look up chart;  $\Delta v$  and Effective-g as blast load descriptors along with duration of blast pulse

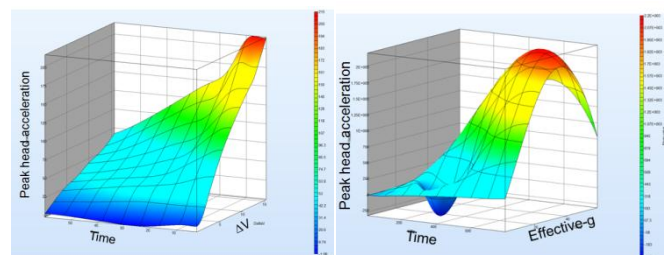
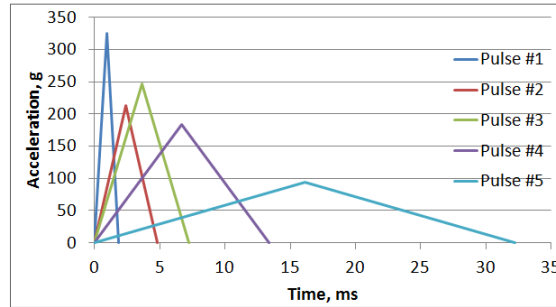


Fig 24 a & b: An example injury response surface in 3D

**Blast injury predictor tool**

From the linear/quadratic regression equations resulting from this parametric study, occupant injuries for any triangular-shaped pulse (within a certain range of  $0 \leq \Delta v \leq 15$  m/s) can be easily computed. A simple macro-enabled tool has been built using Microsoft Excel<sup>®</sup> and shown in Table A4. Users can simply select and input two key blast descriptors such as peak acceleration and time duration (shown as yellow cells in Table A4-2) and the injury table gets automatically updated (Table A4-3). User inputs can be provided by directly entering in the yellow cells, or by dragging the sliders shown in Table A4-2 to desired values. The injury values as determined by the various appropriate best-fit equations depending on  $T$  are computed, compared against the

reference values and color-coded as low, moderate and high risk. The users have the option of setting the reference values per their specific program needs/targets. Results are shown for all three seat types as well. In addition, users can also choose the factor  $r$  (default value of 0.05) to determine effective-g for the chosen pulse which also gets updated and displayed graphically as shown in Table A4-1.



**Fig 25:** Various pulse shapes arbitrarily chosen to verify the validity of the predictor tool

**Table 2:** Arbitrarily chosen pulses to verify the validity of the predictor tool

| Pulse # | Peak, Dec., g | Duration, ms | $\Delta V$ , m/s | Eff-g  | Sp. Power |
|---------|---------------|--------------|------------------|--------|-----------|
| 1       | 324.43        | 1.85         | 2.94             | 213.51 | 955.11    |
| 2       | 212.40        | 4.80         | 5.00             | 139.78 | 1062.15   |
| 3       | 246.90        | 7.23         | 8.76             | 162.48 | 2161.82   |
| 4       | 183.63        | 13.40        | 12.07            | 120.85 | 2216.31   |
| 5       | 94.32         | 32.23        | 14.91            | 62.07  | 1406.39   |

To demonstrate the accuracy and efficiency of this tool, five arbitrary pulses as shown in Figure 25 and Table 2 were selected which were not in the original seed simulations of the parametric M&S study, to determine injuries as predicted by the Blast predictor tool against corresponding results from the direct MADYMO<sup>®</sup> simulations. Table 3 shows typical injuries and values from the tool as well as from the direct simulations. The maximum error was within a range of  $\pm 10\%$  except for those cases when the injury magnitude is very low or very high, e.g., HIC<sub>15ms</sub> for Pulse #1 and #5 respectively. This clearly shows that the developed tool has enormous advantages as a reduced order modeling tool, taking merely a few seconds to predict the injuries correctly as opposed to requiring expensive M&S software, over 20 minutes of computation time, followed by post-processing, plotting, tabulation, etc by an expert user/analyst.

**Table 3:** Comparison of injury values obtained from the RBD model to those obtained from the predictor tool

| Occupant Injury                           | Pulse #1 |           |        | Pulse #2 |           |        | Pulse #3 |           |        | Pulse #4 |           |        | Pulse #5 |           |        |
|---|----------|-----------|--------|----------|-----------|--------|----------|-----------|--------|----------|-----------|--------|----------|-----------|--------|
|   | M&S      | Predicted | % diff | M&S      | Predicted | % diff | M&S      | Predicted | % diff | M&S      | Predicted | % diff | M&S      | Predicted | % diff |
| Head resultant acceleration 2ms-clip, g   | 41.1     | 41.6      | 1%     | 70.6     | 66.4      | -6%    | 113.3    | 112.9     | 0%     | 127.7    | 126.4     | -1%    | 114.6    | 115.0     | 0%     |
| Peak Head resultant acceleration, g       | 43.4     | 45.0      | 4%     | 76.1     | 71.0      | -7%    | 122.3    | 120.1     | -2%    | 139.8    | 133.4     | -5%    | 121.1    | 120.8     | 0%     |
| HIC 15                                    | 49.7     | 13.0      | -74%   | 163.7    | 147.0     | -10%   | 710.5    | 743.0     | 5%     | 1420.6   | 1336.0    | -6%    | 1105.1   | 1230.0    | 11%    |
| Nij                                       | 0.3      | 0.3       | 0%     | 0.6      | 0.6       | -3%    | 1.0      | 1.0       | 3%     | 1.2      | 1.2       | -2%    | 1.2      | 1.2       | -2%    |
| Chest resultant acceleration, 3ms clip, g | 39.3     | 42.0      | 7%     | 69.9     | 68.8      | -2%    | 109.8    | 113.0     | 3%     | 120.2    | 114.2     | -5%    | 106.9    | 109.8     | 3%     |
| DRI                                       | 13.8     | 14.0      | 1%     | 22.0     | 22.0      | 0%     | 37.2     | 37.0      | 0%     | 50.7     | 50.0      | -1%    | 58.1     | 59.0      | 2%     |
| Peak Lumbar Compression, kN               | -8.6     | -9.2      | 7%     | -15.6    | -15.1     | -3%    | -26.5    | -26.3     | -1%    | -29.6    | -27.5     | -7%    | -21.2    | -21.9     | 4%     |

**Effect of loading path on injuries**

A separate but related study was also conducted to observe the effect of *shape* of the pulse on occupant injuries, keeping  $\Delta v$  and duration  $T$  constant. Eight different shapes were considered including haversine, sine and others as shown in Fig 26 and three time durations of 5, 10 and 40 ms (only 5 ms case shown in Fig 26). The resulting occupant injuries monitored throughout this study are presented in Tables A5-A7 for 5, 10 and 40 ms, respectively. The following observations may be made from these tables:

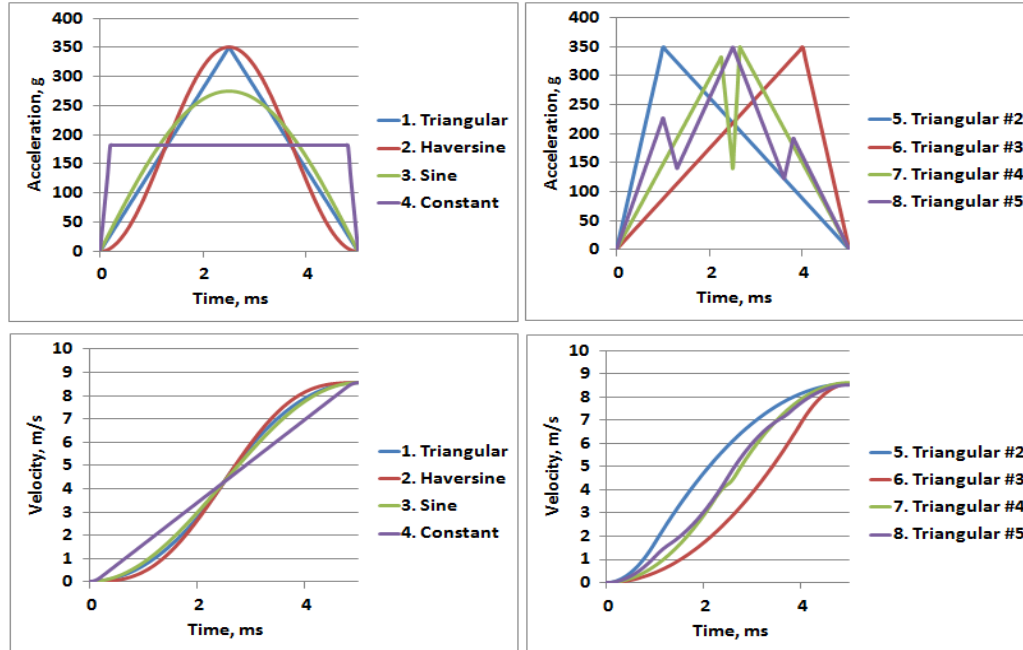


**Fig 26:** Various pulse shapes studied; acceleration profiles at the top and corresponding velocity profiles at the bottom

- (1) The coefficient of variation for each of the ten injury parameters resulting when the model is subjected to these eight pulses of varied shape (but keeping  $\Delta v$  and duration  $T$  constant) is less than 5% for most injuries for  $T < 10$  ms, and less than 10% even for  $T = 40$  ms.
- (2) These low values show that for any given  $\Delta v$ , not only the shape of the pulse, but also its peak magnitude ( $G_{peak}$ ) and duration ( $T$ ) do not play a major role in the severity of occupant injury, when the duration of the pulses are in the blast loading range of  $T < 10$ ms.
- (3) It can also be seen from the Table A7 that even when the duration of the pulse is extended to 40 ms, the coefficient of variation still did not exceed more than 10% for majority of the occupant injuries considered in this study.
- (4) The non-dependence of the occupant injuries on loading paths as long as the  $\Delta v$  is reached in a specified time duration  $T$  is an important finding because medical researchers, seat designers, etc., utilize different physical devices to enforce blast-like loading pulses to occupants, which may result in different loading paths and rates to obtain the desired  $\Delta v$ ; nevertheless, this study indicates that the injuries produced in the ATD will still be substantially the same, as long as the duration of loading  $T$  is short and in the range of typical blast events (0-10 ms).

## CONCLUSIONS

The following broad conclusions may be made from the analysis, results and discussions of the preceding sections:

- (1) No single blast loading parameter from an input pulse can be used to fully determine the occupant injury risk over the entire wide range of pulse durations (0-60ms).
- (2) Among the different blast pulse parameters considered in this study,  $\Delta v$  is the best single indicator for estimating injury criteria, for typical blast pulse duration ranges (0-20 ms), independent of seat type.
- (3) For vehicle designs where the input pulse to the occupant gets stretched to longer duration pulses (30-60 ms), for example, with isolated floors, EA structural hulls, etc., the other two metrics considered in this study, namely, Effective G and Specific Power seem to possess higher potential to be the best single indicator and predictor of occupant injuries.
- (4) For a given  $\Delta v$  and  $T$ , the shape of the pulse and its peak value has no significant effect on the injury criteria, again for typical blast pulse duration ranges, an important finding for design of test setups.
- (5) Occupant injury trends observed in this study strongly agree with physical test data.

- (6) An easy-to-use, rapid injury estimator tool was constructed in Microsoft Excel<sup>®</sup> as a function of duration  $T$ , and  $G_{peak}$ , from the occupant injury regression trends obtained from this parametric study. This tool will enable decision makers arrive at informed decisions during early concept design stages, Analysis of Alternatives (AoA) studies, etc. This tool takes mere seconds to arrive at the injury predictions when compared to a minimum 20 minutes required by the direct method (using expensive software and hardware) with additional time required for post-processing, plotting, and tabulation, etc.
- (7) It is noteworthy that these results are only representative of the underlying power of the technology. By extending this methodology to one or more seats with the EA as one of the design variables, family of better validated ATDs of different sizes, new and improved injury criteria from the bio-medical research the tool can be made extremely useful in ground vehicle acquisition.
- (8) The methodology used in this project is being planned for extended use elsewhere in the Army for data from physical drop tower/vertical sled tests, as well as from Live-Fire blast tests to develop similar empirically-based tools for use by designers, program managers, evaluators, etc.

#### DISCLAIMER

Reference herein to any specific commercial company, product, process, or service by trade name, trademark, manufacturer, or otherwise does not necessarily constitute or imply its endorsement, recommendation, or favoring by the United States Government or the Dept. of the Army (DoA). The opinions of the authors expressed herein do not necessarily state or reflect those of the United States Government or the DoD, and shall not be used for advertising or product endorsement purposes.

#### ACKNOWLEDGMENTS

The authors would like to thank the Underbody Blast Modeling/Methodology (UBM) program managed by ARL/SLAD and ATEC, for the provided funding which made this project possible. This material is based on R&D work supported by the U.S. Army TACOM Life Cycle Command under Contract No. W56HZV-08-C-0236, through a subcontract with Mississippi State University (MSU), and was performed for the Simulation Based Reliability and Safety (SimBRS) research program. Any opinions, finding and conclusions or recommendations in this paper are those of the author(s) and do not necessarily reflect the views of the U.S. Army TACOM Life Cycle Command.

The authors are also most grateful to Mr. Sudhakar Arepally for his reviews of this work, and for patiently providing insight to his earlier research on Effective-G [13] which served as the precursor for this project.

#### GLOSSARY

|                     |   |
|---------------------|---|
| AoA                 | Analysis of Alternatives  |
| ATD                 | Anthropomorphic Test Device   |
| ATEC                | Army Test and Evaluation Command  |
| ARL                 | Army Research Labs  |
| COTS                | Commercial-Off-The-Shelf  |
| DoA                 | Department of the Army  |
| DoD                 | Department of Defense   |
| DRI                 | Dynamic Response Index  |
| DTIC                | Defense Technical Information Center, <a href="https://www.dtic.mil/">https://www.dtic.mil/</a> |
| $\Delta v$          | Delta-V   |
| EA                  | Energy Absorbing  |
| FE/FEA              | Finite Element / Finite Element Analysis  |
| $G_{avg}$           | Average acceleration of pulse   |
| $G_{eff}$           | Effective-G   |
| $G_{peak}$          | Peak acceleration value of pulse  |
| HIC                 | Head Impact Criterion   |
| IED                 | Improvised Explosive Device   |
| LSDYNA <sup>®</sup> | COTS structural dynamics software from Lawrence Livermore Software Corporation, CA              |
| LSOPT <sup>®</sup>  | COTS optimization software from Lawrence Livermore Software Corporation, CA                     |
| MADYMO <sup>®</sup> | MAThematical DYnamic Models, COTS multibody dynamics software from TASS, Netherlands            |
| MRAP                | Mine-Resistant Ambush Protected   |
| ms/msec             | milliseconds  |

|          |  |
|----------|--|
| M&S      | Modeling & Simulation  |
| MSU      | Mississippi State University                                 |
| MB/RMB   | Multi-body/Rigid Multi-body                                  |
| $N_{ij}$ | Neck Injury Criterion  |
| $r_c$    | Correlation Coefficient                                      |
| R&D      | Research & Development                                       |
| RO/ROM   | Reduced Order / Reduced Order Model                          |
| SimBRS   | Simulation Based Reliability and Safety                      |
| SLAD     | Survivability and Lethality Analysis Directorate             |
| SP       | Specific Power   |
| TACOM    | Tank Command   |
| TARDEC   | Tank Automotive Research, Development and Engineering Center |
| TASS     | TNO Automotive Safety Solutions division                     |
| UBM      | Underbody Blast Modeling/Methodology                         |

## REFERENCES

- [1] Wilson. C., "Improvised Explosive Devices (IEDs) in Iraq and Afghanistan: Effects and Countermeasures", CRS Report for Congress, RS22330, 28 August 2007.
- [2] Bird, S., and Fairweather. C., "Recent military fatalities in Afghanistan (and Iraq) by cause and nationality", MRC Biostatistics Unit, UK, February 2010.
- [3] Farago. J., "IED Casualties in Afghanistan Soaring", <http://www.newser.com/story/55161/ied-casualties-inafghanistan-soaring.html> , 3 April 2009.
- [4] Thyagarajan, R., "End-to-end System level M&S tool for Underbody Blast Events", 27th Army Science Conference, Army Technology Showcase, Orlando, FL, Nov 29 – Dec 2. DTIC Report # ADA550921, TARDEC Registration # 21365, 2000
- [5] Weed, R., Moore, C., Thyagarajan, R., "Enhancements and Analysis of CTH Software for Underbody Blast", DTIC Report # ADA571176, TARDEC Registration # 23676, 2013
- [6] Vlahopoulos, N. Zhang, G, "Validation of a Simulation Process for Assessing the Response of a Vehicle and Its Occupants to an Explosive Threat", 27th Army Science Conference, Orlando, FL, 2010
- [7] Moral, R., Danielson, K., and Ehr Gott, J., "Tactical Wheeled Vehicle Survivability: Comparison of Explosive-Soil-Air-Structure Simulations to Experiments Using the Impulse Measurement Device," Army Corp of Engineers Technical Report ERDC/GSL TR-10-27, August, 2010
- [8] Kerley, G., "Numerical Modeling of Buried Mine Explosions", ARL-CR-461, Army Research Laboratory, Aberdeen Proving Ground, MD, 2001
- [9] Williams, K., McClennan, S., Durocher, R, St-Jean, B., Tremblay, J., "Validation of a Loading Model for Simulating Blast Mine Effects on Armoured Vehicles," 7th International LS-DYNA Users Conference, Detroit, MI 2002
- [10] Williams, K., McClennan S., "A numerical analysis of mine blast effects on simplified target geometries: Validation of loading models," Defense R&D Canada-Valcartier, DRDC Valcartier TM 2002-260, 2002
- [11] Dooge, D., Dwarampudi, R., Schaffner, G., Miller, A., Thyagarajan, R., Vunnam, M., Babu, V., "Evolution of Occupant Survivability Simulation Framework Using FEM-SPH Coupling," 2011 NDIA Ground Vehicle System Engineering and Technology Symposium (GVSETS), MSTV Mini-Symposium Paper, Dearborn, Michigan, August 9-11, 2011
- [12] Final Report of HFM-090 Task Group 25, "Test Methodology for Protection of Vehicle Occupants against Anti-Vehicular Landmine Effects", NATO RTO TECHNICAL REPORT TR-HFM-090, April 2007
- [13] Arepally, S., Gorsich, D., Hope, K., Gentner, S., and Dortleff, K., "Application of mathematical modeling in potentially survivable blast threats in military vehicles", 26th Army Science Conference, Orlando, FL, 1-4 December 2008, DTIC Report# ADA496843
- [14] Rangarajan, N., Moore, J., Gromowski, P., Rinaldi, J., Yoganandan, N., Pintar, F., Mariman, D., and McEntire, J., "Response of dummies to high onset rate Gz loading on sled", *unpublished report*.
- [15] Sheng, J. and Arepally, S., "Crew Injury Risk Assessment – Effective g vs. Delta V", *Internal TARDEC brief*, December 2009



APPENDIX

**Table A1:** Correlation coefficients between injury parameters and blast indicators/descriptors for triangular pulses (0 ≤ T ≤ 10ms)

|   | Correlation Coefficients |       |       |                |       |       |       |       |       |
|---|--------------------------|-------|-------|----------------|-------|-------|-------|-------|-------|
|   | T from 0-10ms            |       |       |                |       |       |       |       |       |
|   | G-average                |       |       | Specific power |       |       | ΔV    |       |       |
|   | Rigid                    | EA1   | EA2   | Rigid          | EA1   | EA2   | Rigid | EA1   | EA2   |
| 1 HIC @15ms                             | 0.67                     | 0.52  | 0.59  | 0.81           | 0.74  | 0.74  | 0.94  | 0.74  | 0.89  |
| 2 Head resultant acceleration @2ms      | 0.73                     | 0.63  | 0.65  | 0.79           | 0.77  | 0.77  | 1.00  | 0.85  | 0.96  |
| 3 Head resultant acceleration @0ms      | 0.73                     | 0.62  | 0.66  | 0.78           | 0.78  | 0.78  | 1.00  | 0.85  | 0.96  |
| 4 Neck injury criteria, N <sub>ij</sub> | 0.71                     | 0.61  | 0.65  | 0.79           | 0.77  | 0.77  | 1.00  | 0.84  | 0.95  |
| 5 Chest resultant acceleration @3ms     | 0.74                     | 0.63  | 0.62  | 0.78           | 0.74  | 0.74  | 0.99  | 0.87  | 0.94  |
| 6 Chest resultant acceleration @7ms     | 0.65                     | 0.57  | 0.73  | 0.72           | 0.80  | 0.80  | 0.96  | 0.83  | 0.95  |
| 7 Lumbar spine compression @30ms        | 0.59                     | -0.42 | 0.19  | 0.53           | 0.40  | 0.40  | 0.77  | -0.65 | 0.30  |
| 8 Lumbar spine compression @0ms         | -0.75                    | -0.66 | -0.68 | -0.80          | -0.81 | -0.81 | -1.00 | -0.88 | -0.96 |
| 9 Pelvis vertical acceleration @7ms     | -0.46                    | -0.23 | -0.13 | -0.63          | -0.08 | -0.08 | -0.74 | -0.58 | -0.22 |
| 10 DRI (Z)                              | 0.71                     | 0.71  | 0.70  | 0.78           | 0.80  | 0.80  | 1.00  | 0.99  | 0.99  |

|  |                |
|--|----------------|
|  | 0.5 < r < 0.75 |
|  | 0.75 < r < 0.9 |
|  | r > 0.9        |

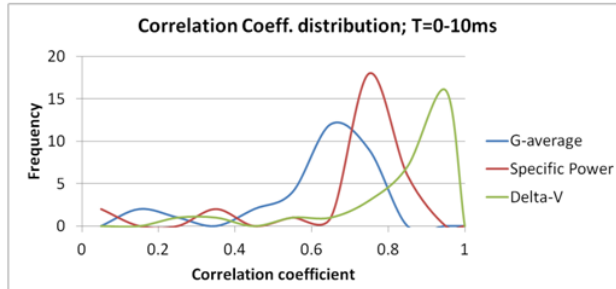


**Table A2:** Correlation coefficients between injury parameters and blast indicators/descriptors for triangular pulses (10 ≤ T ≤ 20ms)

|   | Correlation Coefficients |       |       |                |       |       |       |       |       |
|---|--------------------------|-------|-------|----------------|-------|-------|-------|-------|-------|
|   | T from 10-20ms           |       |       |                |       |       |       |       |       |
|   | G-average                |       |       | Specific power |       |       | ΔV    |       |       |
|   | Rigid                    | EA1   | EA2   | Rigid          | EA1   | EA2   | Rigid | EA1   | EA2   |
| 1 HIC @15ms                             | 0.94                     | 0.73  | 0.86  | 0.99           | 0.85  | 0.95  | 0.95  | 0.75  | 0.90  |
| 2 Head resultant acceleration @2ms      | 0.98                     | 0.83  | 0.92  | 0.98           | 0.92  | 0.96  | 0.99  | 0.85  | 0.96  |
| 3 Head resultant acceleration @0ms      | 0.99                     | 0.82  | 0.92  | 0.97           | 0.92  | 0.96  | 0.99  | 0.85  | 0.96  |
| 4 Neck injury criteria, N <sub>ij</sub> | 0.97                     | 0.81  | 0.92  | 0.98           | 0.92  | 0.97  | 0.99  | 0.84  | 0.96  |
| 5 Chest resultant acceleration @3ms     | 0.99                     | 0.84  | 0.92  | 0.94           | 0.93  | 0.98  | 0.98  | 0.87  | 0.96  |
| 6 Chest resultant acceleration @7ms     | 0.94                     | 0.90  | 0.95  | 0.96           | 0.89  | 0.91  | 0.98  | 0.89  | 0.93  |
| 7 Lumbar spine compression @30ms        | 0.92                     | -0.77 | 0.09  | 0.84           | -0.66 | 0.29  | 0.86  | -0.82 | 0.04  |
| 8 Lumbar spine compression @0ms         | -0.99                    | -0.84 | -0.92 | -0.96          | -0.94 | -0.97 | -0.98 | -0.88 | -0.96 |
| 9 Pelvis vertical acceleration @7ms     | -0.67                    | -0.55 | -0.04 | -0.62          | -0.47 | 0.10  | -0.76 | -0.56 | -0.06 |
| 10 DRI (Z)                              | 0.96                     | 0.95  | 0.94  | 0.96           | 0.97  | 0.97  | 1.00  | 0.98  | 0.98  |

|  |                |
|--|----------------|
|  | 0.5 < r < 0.75 |
|  | 0.75 < r < 0.9 |
|  | r > 0.9        |

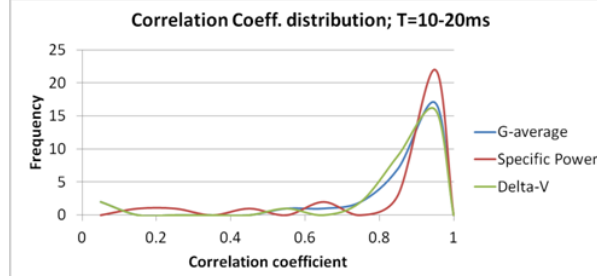


**Table A3:** Correlation coefficients between injury parameters and blast indicators/descriptors for triangular pulses ( $20 \leq T \leq 60\text{ms}$ )

|   | Correlation Coefficients |       |       |                |       |       |       |       |       |
|---|--------------------------|-------|-------|----------------|-------|-------|-------|-------|-------|
|   | T from 20-60ms           |       |       |                |       |       |       |       |       |
|   | G-average                |       |       | Specific power |       |       | ΔV    |       |       |
|   | Rigid                    | EA1   | EA2   | Rigid          | EA1   | EA2   | Rigid | EA1   | EA2   |
| 1 HIC @15ms                             | 0.96                     | 0.69  | 0.82  | 0.98           | 0.77  | 0.93  | 0.77  | 0.53  | 0.82  |
| 2 Head resultant acceleration @2ms      | 0.98                     | 0.79  | 0.88  | 0.98           | 0.88  | 0.96  | 0.86  | 0.68  | 0.92  |
| 3 Head resultant acceleration @0ms      | 0.98                     | 0.79  | 0.87  | 0.98           | 0.88  | 0.96  | 0.85  | 0.68  | 0.92  |
| 4 Neck injury criteria, N <sub>ij</sub> | 0.98                     | 0.79  | 0.88  | 0.99           | 0.88  | 0.96  | 0.84  | 0.69  | 0.92  |
| 5 Chest resultant acceleration @3ms     | 0.97                     | 0.80  | 0.86  | 0.98           | 0.90  | 0.95  | 0.88  | 0.74  | 0.92  |
| 6 Chest resultant acceleration @7ms     | 0.96                     | 0.90  | 0.69  | 0.98           | 0.93  | 0.76  | 0.92  | 0.85  | 0.89  |
| 7 Lumbar spine compression @30ms        | 0.16                     | -0.69 | -0.28 | 0.00           | -0.67 | -0.21 | -0.41 | -0.86 | -0.40 |
| 8 Lumbar spine compression @0ms         | -0.99                    | -0.79 | -0.84 | -0.96          | -0.89 | -0.93 | -0.84 | -0.74 | -0.95 |
| 9 Pelvis vertical acceleration @7ms     | -0.91                    | -0.69 | -0.08 | -0.94          | -0.70 | 0.02  | -0.94 | -0.79 | -0.15 |
| 10 DRI (Z)                              | 0.89                     | 0.90  | 0.86  | 0.93           | 0.95  | 0.94  | 0.99  | 0.95  | 0.96  |

|  |                |
|--|----------------|
|  | 0.5 < r < 0.75 |
|  | 0.75 < r < 0.9 |
|  | r > 0.9        |

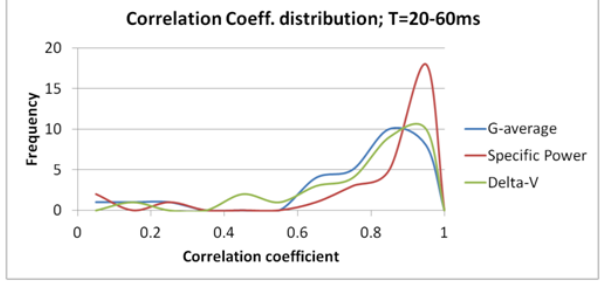
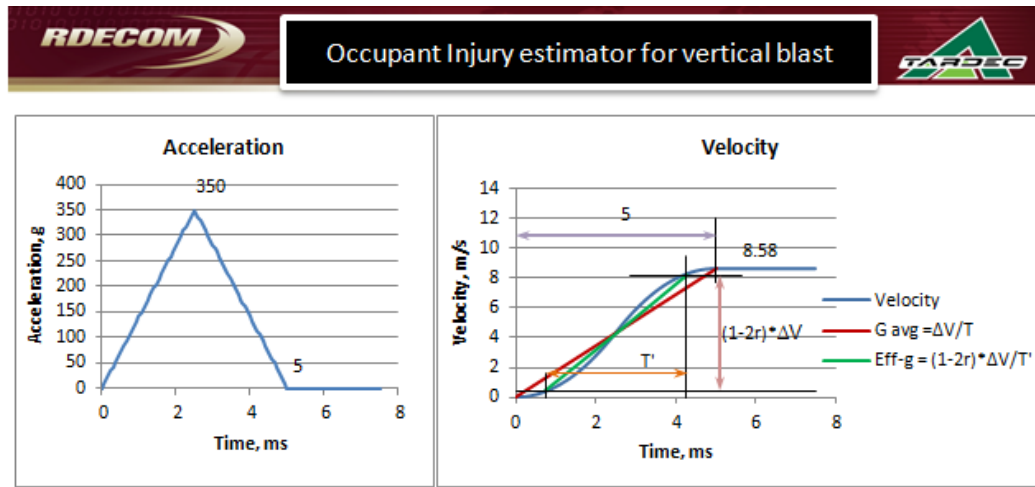


**Table A4-1 A4-2:** Blast injury predictor tool



Enter the value of time duration of pulse in milliseconds, and peak acceleration in g's in the yellow shaded cells. Conversely you can use the arrow buttons to desired values such that  $1.5 \leq \Delta V \leq 15$  m/s. Please note that the solution range is only valid for the following ranges;

$1.0 \leq T \leq 60$   
 $10 \leq G_{peak} \leq 1200$

| # | Blast load parameters                              | Value |
|---|--|-------|
| 1 | Peak acceleration in g's, $G_{peak}$               | 350   |
| 2 | Time duration of pulse, T, ms                      | 5     |
| 3 | "r" factor, % (default 5%)                         | 5     |
| 4 | $\Delta V$ , m/s                                   | 8.58  |
| 5 | Adjusted $\Delta V$ for effective-g, m/s           | 7.73  |
| 6 | Adjusted time for effective-g, ms                  | 3.419 |
| 7 | G-Average = $(G_{peak} / 2)$                       | 175   |
| 8 | Effective-g = $G_{Average} \times (1 + \sqrt{2r})$ | 230   |

| # | Occupant Injury Criteria              |   | Seat EA system |            |              |
|---|---------------------------------------|---|----------------|------------|--------------|
|   | Criteria                              | Reference values                          | None           | EA1 (15kN) | EA2 (7.5 kN) |
| 1 | HIC@15ms                              | 350, 700, 1050 (Low, moderate, high risk) | 705            | 29         | 384          |
| 2 | Head resultant acceleration (2ms cl)  | 150g                                      | 110.8          | 33.9       | 89.8         |
| 3 | Head resultant acceleration (Peak)    | 180g                                      | 117.9          | 36.2       | 95.1         |
| 4 | Neck injury criteria, Nij             | <1  | 0.97           | 0.25       | 0.77         |
| 5 | Chest resultant acceleration (3ms cl) | 60g                                       | 111.2          | 34.1       | 76.3         |
| 6 | Lumbar spine compression (Peak)       | 6672 N                                    | 25,773         | 8,103      | 17,433       |
| 7 | DRI <sub>2</sub>                      | 15, 18, 23 (low, moderate, high risk)     | 37             | 30         | 32           |

**Table A5:** Variations in occupant injuries when the model is subjected to pulses of varied shape (T = 5ms; Δv = 8.6 m/s)

**T = 5ms**

| Pulse iterations |               |              |              |                     |         |         |        |       | HEAD                      |       |         | NECK | CHEST           |                           | PELVIS |                   | LUMBAR SPINE |                       |       |
|------------------|---------------|--------------|--------------|---------------------|---------|---------|--------|-------|---------------------------|-------|---------|------|-----------------|---------------------------|--------|-------------------|--------------|-----------------------|-------|
| #                | Pulse type    | Peak Dec., g | Duration, ms | Rate of onset, g/ms | ΔV, m/s | Sp. Pwr | Eff. G | G-avg | Resultant acceleration, g |       |         | HIC  | N <sub>ij</sub> | Resultant acceleration, g |        | Z-Acceleration, g | DRI (z), g   | Axial compression, kN |       |
|                  |               |              |              |                     |         |         |        |       | @ 2ms                     | @ 0ms | @ 15 ms |      |                 | CFC 1000                  | @ 3ms  |                   |              | @ 7ms                 | @ 7ms |
| 1                | Triangular    | 350          | 5            | 140                 | 8.6     | 3004    | 218    | 175   | 113.4                     | 122.7 | 687     | 0.96 | 111.2           | 33.9                      | -4.9   | 36.4              | 0.0          | -26.5                 |       |
| 2                | Haversine     | 350          | 5            | 140                 | 8.6     | 3003    | 235    | 175   | 113.6                     | 122.9 | 689     | 0.96 | 111.7           | 34.9                      | -4.8   | 36.4              | 0.0          | -26.5                 |       |
| 3                | Sine          | 275          | 5            | 110                 | 8.6     | 2360    | 210    | 175   | 113.2                     | 122.5 | 679     | 0.96 | 110.7           | 32.6                      | -4.8   | 36.2              | 0.0          | -26.4                 |       |
| 4                | Constant      | 182          | 5            | NA                  | 8.6     | 1562    | 181    | 175   | 112.5                     | 121.5 | 673     | 0.96 | 109.1           | 30.5                      | -4.9   | 36.3              | 0.0          | -26.3                 |       |
| 5                | Triangular #2 | 350          | 5            | 140                 | 8.6     | 3004    | 212    | 175   | 113.8                     | 123.1 | 689     | 0.97 | 111.3           | 33.8                      | -4.9   | 36.4              | 0.0          | -26.5                 |       |
| 6                | Triangular #3 | 350          | 5            | 140                 | 8.6     | 3004    | 212    | 175   | 112.9                     | 122.1 | 683     | 0.96 | 110.6           | 32.7                      | -4.9   | 36.4              | 0.0          | -26.4                 |       |
| 7                | Triangular #4 | 350          | 5            | 140                 | 8.6     | 3004    | 217    | 175   | 114.0                     | 123.4 | 701     | 0.97 | 111.7           | 33.8                      | -5.0   | 36.6              | 0.0          | -26.6                 |       |
| 8                | Triangular #5 | 350          | 5            | 140                 | 8.6     | 3004    | 205    | 175   | 112.9                     | 122.1 | 673     | 0.96 | 110.3           | 33.0                      | -4.9   | 36.2              | 0.0          | -26.3                 |       |

| Including "Constant" type pulse              |     |      |       |       |       |       |       |     |       |      |      |      |     |       |
|--|-----|------|-------|-------|-------|-------|-------|-----|-------|------|------|------|-----|-------|
| Mean, μ =                                    | 8.6 | 2743 | 211.2 | 175.0 | 113.3 | 122.5 | 684.3 | 1.0 | 110.8 | 33.2 | -4.9 | 36.4 | 0.0 | -26.4 |
| Standard deviation, σ =                      | 0.0 | 528  | 15.1  | 0.0   | 0.5   | 0.6   | 9.4   | 0.0 | 0.9   | 1.3  | 0.1  | 0.1  | 0.0 | 0.1   |
| Coefficient of variation, C <sub>v</sub> (%) | 0%  | 19%  | 7%    | 0%    | 0%    | 1%    | 1%    | 0%  | 1%    | 4%   | 1%   | 0%   | 0%  | 0%    |

| Excluding "Constant" type pulse              |     |        |       |       |       |       |       |     |       |      |      |      |     |       |
|--|-----|--------|-------|-------|-------|-------|-------|-----|-------|------|------|------|-----|-------|
| Mean, μ =                                    | 8.6 | 2912.0 | 215.4 | 175.0 | 113.4 | 122.7 | 685.9 | 1.0 | 111.1 | 33.5 | -4.9 | 36.4 | 0.0 | -26.5 |
| Standard deviation, σ =                      | 0.0 | 243.6  | 9.8   | 0.0   | 0.4   | 0.5   | 8.9   | 0.0 | 0.5   | 0.8  | 0.1  | 0.1  | 0.0 | 0.1   |
| Coefficient of variation, C <sub>v</sub> (%) | 0%  | 8%     | 5%    | 0%    | 0%    | 0%    | 1%    | 1%  | 0%    | 2%   | 1%   | 0%   | 0%  | 0%    |

**Table A6:** Variations in occupant injuries when the model is subjected to pulses of varied shape (T = 10ms; Δv = 8.6 m/s)

**T = 10ms**

| Pulse iterations |               |              |              |                     |         |         |        |       | HEAD                      |       |         | NECK | CHEST           |                           | PELVIS |                   | LUMBAR SPINE |                       |       |
|------------------|---------------|--------------|--------------|---------------------|---------|---------|--------|-------|---------------------------|-------|---------|------|-----------------|---------------------------|--------|-------------------|--------------|-----------------------|-------|
| #                | Pulse type    | Peak Dec., g | Duration, ms | Rate of onset, g/ms | ΔV, m/s | Sp. Pwr | Eff. G | G-avg | Resultant acceleration, g |       |         | HIC  | N <sub>ij</sub> | Resultant acceleration, g |        | Z-Acceleration, g | DRI (z), g   | Axial compression, kN |       |
|                  |               |              |              |                     |         |         |        |       | @ 2ms                     | @ 0ms | @ 15 ms |      |                 | CFC 1000                  | @ 3ms  |                   |              | @ 7ms                 | @ 7ms |
| 1                | Triangular    | 175          | 10           | 35                  | 8.6     | 1502    | 109    | 88    | 103.8                     | 111.4 | 628     | 0.88 | 101.0           | 27.8                      | -5.9   | 36.4              | 0.0          | -23.9                 |       |
| 2                | Haversine     | 175          | 10           | 35                  | 8.6     | 1502    | 118    | 88    | 107.1                     | 115.0 | 649     | 0.91 | 103.4           | 28.0                      | -5.5   | 36.4              | 0.0          | -24.9                 |       |
| 3                | Sine          | 138          | 10           | 28                  | 8.6     | 1180    | 105    | 88    | 101.7                     | 109.1 | 621     | 0.86 | 99.3            | 29.9                      | -6.2   | 36.3              | 0.0          | -24.1                 |       |
| 4                | Constant      | 91           | 10           | NA                  | 8.6     | 781     | 91     | 88    | 90.8                      | 98.2  | 582     | 0.78 | 93.3            | 45.1                      | -20.0  | 36.4              | 0.0          | -22.1                 |       |
| 5                | Triangular #2 | 175          | 10           | 35                  | 8.6     | 1502    | 106    | 88    | 102.6                     | 110.1 | 622     | 0.87 | 100.9           | 31.7                      | -4.8   | 36.4              | 0.0          | -24.3                 |       |
| 6                | Triangular #3 | 175          | 10           | 35                  | 8.6     | 1502    | 106    | 88    | 101.8                     | 109.1 | 626     | 0.87 | 98.1            | 28.5                      | -8.5   | 36.5              | 0.0          | -23.9                 |       |
| 7                | Triangular #4 | 175          | 10           | 35                  | 8.6     | 1502    | 108    | 88    | 103.6                     | 111.1 | 638     | 0.88 | 100.9           | 28.6                      | -6.0   | 36.7              | 0.0          | -24.2                 |       |
| 8                | Triangular #5 | 175          | 10           | 35                  | 8.6     | 1502    | 103    | 88    | 100.9                     | 108.4 | 610     | 0.86 | 98.9            | 30.0                      | -6.0   | 36.2              | 0.0          | -23.9                 |       |

| Including "Constant" type pulse              |     |      |       |      |       |       |       |     |      |      |      |      |     |       |
|--|-----|------|-------|------|-------|-------|-------|-----|------|------|------|------|-----|-------|
| Mean, μ =                                    | 8.6 | 1372 | 105.6 | 87.5 | 101.5 | 109.1 | 621.9 | 0.9 | 99.5 | 31.2 | -7.9 | 36.4 | 0.0 | -23.9 |
| Standard deviation, σ =                      | 0.0 | 264  | 7.6   | 0.0  | 4.7   | 4.8   | 19.8  | 0.0 | 3.0  | 5.8  | 5.0  | 0.1  | 0.0 | 0.8   |
| Coefficient of variation, C <sub>v</sub> (%) | 0%  | 19%  | 7%    | 0%   | 5%    | 4%    | 3%    | 4%  | 3%   | 18%  | 64%  | 0%   | 0%  | 3%    |

| Excluding "Constant" type pulse              |     |        |       |      |       |       |       |     |       |      |      |      |     |       |
|--|-----|--------|-------|------|-------|-------|-------|-----|-------|------|------|------|-----|-------|
| Mean, μ =                                    | 8.6 | 1456.0 | 107.7 | 87.5 | 103.1 | 110.6 | 627.6 | 0.9 | 100.4 | 29.2 | -6.1 | 36.4 | 0.0 | -24.2 |
| Standard deviation, σ =                      | 0.0 | 121.8  | 4.9   | 0.0  | 2.1   | 2.2   | 12.5  | 0.0 | 1.8   | 1.4  | 1.1  | 0.2  | 0.0 | 0.4   |
| Coefficient of variation, C <sub>v</sub> (%) | 0%  | 8%     | 5%    | 0%   | 2%    | 2%    | 2%    | 2%  | 2%    | 5%   | 19%  | 0%   | 0%  | 1%    |

**Table A7:** Variations in occupant injuries when the model is subjected to pulses of varied shape (T = 10ms; Δv = 8.6 m/s)

**T = 40ms**

| # | Pulse type    | Pulse iterations |                |                     |          |         |        |       | HEAD                      |       |       | NECK            | CHEST                     |      | PELVIS              |            | LUMBAR                |       |
|---|---------------|------------------|----------------|---------------------|----------|---------|--------|-------|---------------------------|-------|-------|-----------------|---------------------------|------|---------------------|------------|-----------------------|-------|
|   |               | Peak, Dec., g    | Durat- ion, ms | Rate of onset, g/ms | ΔV, m/s  | Sp. Pwr | Eff. G | G-avg | Resultant acceleration, g |       | H I C | N <sub>ij</sub> | Resultant acceleration, g |      | Z-Accele- ration, g | DRI (z), g | Axial compression, kN |       |
|   |               | @ 2ms            | @ 0ms          | @ 15 ms             | CFC 1000 | @ 3ms   | @ 7ms  | @ 7ms | @ 30ms                    | @ 0ms |       |                 |                           |      |                     |            |                       |       |
| 1 | Triangular    | 44               | 40             | 2                   | 8.6      | 376     | 27     | 22    | 54.6                      | 55.4  | 223   | 0.46            | 47.4                      | 42.0 | -31.6               | 33.7       | -1.3                  | -11.4 |
| 2 | Haversine     | 44               | 40             | 2                   | 8.6      | 375     | 29     | 22    | 62.2                      | 63.7  | 274   | 0.53            | 50.0                      | 49.2 | -31.2               | 34.4       | -1.0                  | -12.7 |
| 3 | Sine          | 34               | 40             | 2                   | 8.6      | 295     | 26     | 22    | 50.7                      | 51.2  | 190   | 0.42            | 44.9                      | 42.2 | -28.0               | 33.3       | -1.6                  | -10.7 |
| 4 | Constant      | 23               | 40             | NA                  | 8.6      | 195     | 23     | 22    | 39.4                      | 40.0  | 100   | 0.30            | 35.9                      | 34.4 | -25.0               | 31.4       | -3.5                  | -8.5  |
| 5 | Triangular #2 | 44               | 40             | 2                   | 8.6      | 376     | 27     | 22    | 52.7                      | 54.0  | 221   | 0.45            | 49.3                      | 41.0 | -24.7               | 33.3       | -1.5                  | -11.5 |
| 6 | Triangular #3 | 44               | 40             | 2                   | 8.6      | 376     | 27     | 22    | 50.6                      | 51.0  | 172   | 0.42            | 45.2                      | 44.9 | -30.9               | 33.3       | -1.5                  | -10.1 |
| 7 | Triangular #4 | 44               | 40             | 2                   | 8.6      | 376     | 27     | 22    | 53.6                      | 54.3  | 212   | 0.45            | 46.1                      | 44.1 | -31.3               | 33.8       | -1.4                  | -11.2 |
| 8 | Triangular #5 | 44               | 40             | 2                   | 8.6      | 376     | 26     | 22    | 52.4                      | 53.6  | 183   | 0.43            | 40.9                      | 39.8 | -30.8               | 33.1       | -1.7                  | -10.8 |

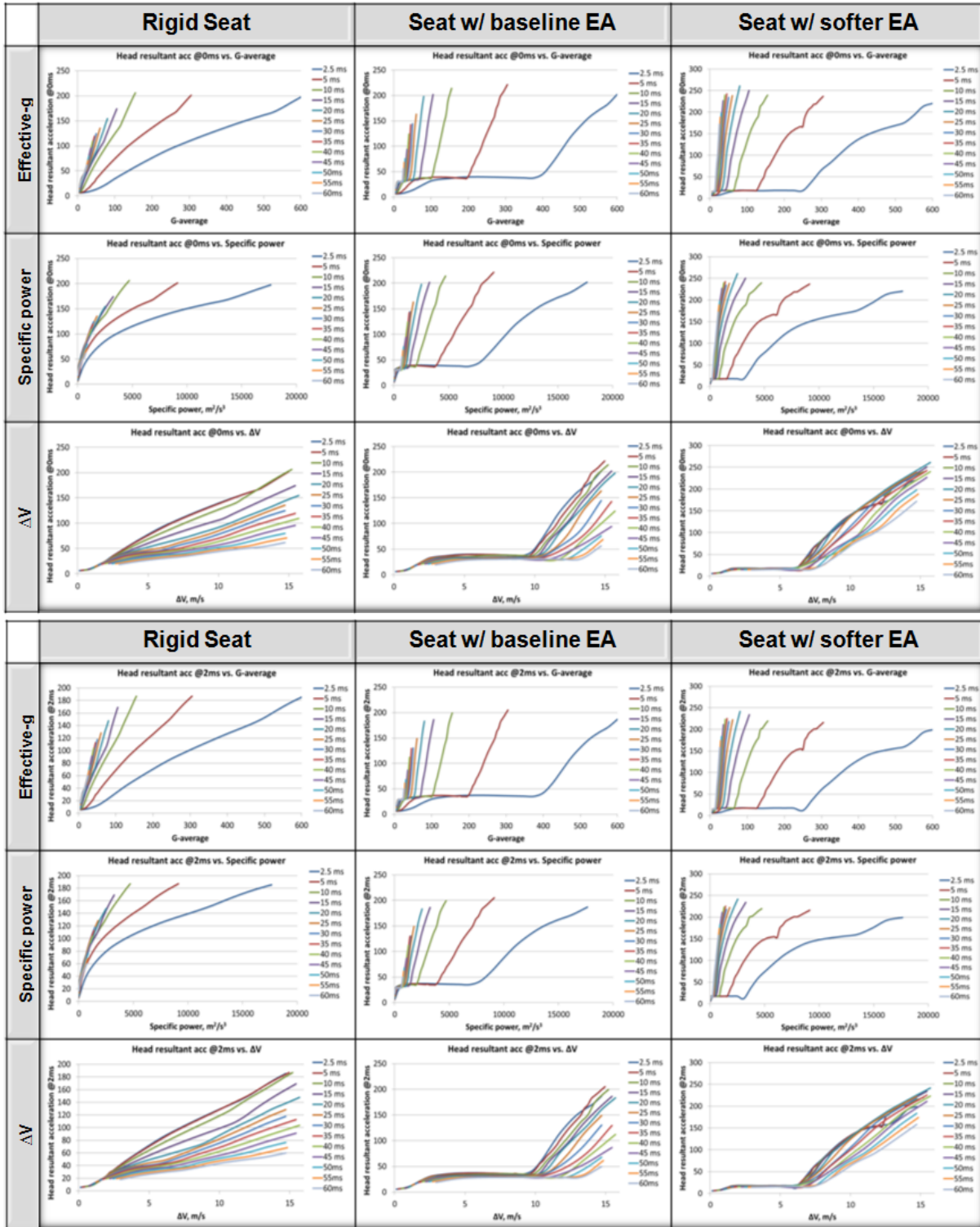
Including "Constant" type pulse

|  |     |     |      |      |      |      |       |     |      |      |       |      |      |       |
|--|-----|-----|------|------|------|------|-------|-----|------|------|-------|------|------|-------|
| Mean, μ =                                    | 8.6 | 343 | 26.4 | 21.9 | 52.0 | 52.9 | 196.9 | 0.4 | 45.0 | 42.2 | -29.2 | 33.3 | -1.7 | -10.9 |
| Standard deviation, σ =                      | 0.0 | 66  | 1.9  | 0.0  | 6.3  | 6.5  | 50.3  | 0.1 | 4.6  | 4.3  | 2.9   | 0.9  | 0.8  | 1.2   |
| Coefficient of variation, C <sub>v</sub> (%) | 0%  | 19% | 7%   | 0%   | 12%  | 12%  | 26%   | 15% | 10%  | 10%  | 10%   | 3%   | 45%  | 11%   |

Excluding "Constant" type pulse

|  |     |       |      |      |      |      |       |     |      |      |       |      |      |       |
|--|-----|-------|------|------|------|------|-------|-----|------|------|-------|------|------|-------|
| Mean, μ =                                    | 8.6 | 364.0 | 26.9 | 21.9 | 53.8 | 54.7 | 210.7 | 0.5 | 46.3 | 43.3 | -29.8 | 33.6 | -1.4 | -11.2 |
| Standard deviation, σ =                      | 0.0 | 30.5  | 1.2  | 0.0  | 4.0  | 4.3  | 34.1  | 0.0 | 3.1  | 3.1  | 2.5   | 0.4  | 0.2  | 0.8   |
| Coefficient of variation, C <sub>v</sub> (%) | 0%  | 8%    | 5%   | 0%   | 7%   | 8%   | 16%   | 8%  | 7%   | 7%   | 9%    | 1%   | 16%  | 7%    |

**Table A10-1, A10-2:** Peak head acceleration (Top) and 2ms clip (Bottom) vs. blast loading parameters for three different seat types



Evaluating the Effectiveness of Various Blast Loading Descriptors as Occupant Injury Predictors... Kulkarni et. al  
 UNCLASSIFIED: Distribution Statement A. Approved for public release.

**Table A10-3, A10-4:**  $N_{ij}$  and Chest resultant acceleration 3ms clip (Bottom) vs. blast loading parameters for three different seat types

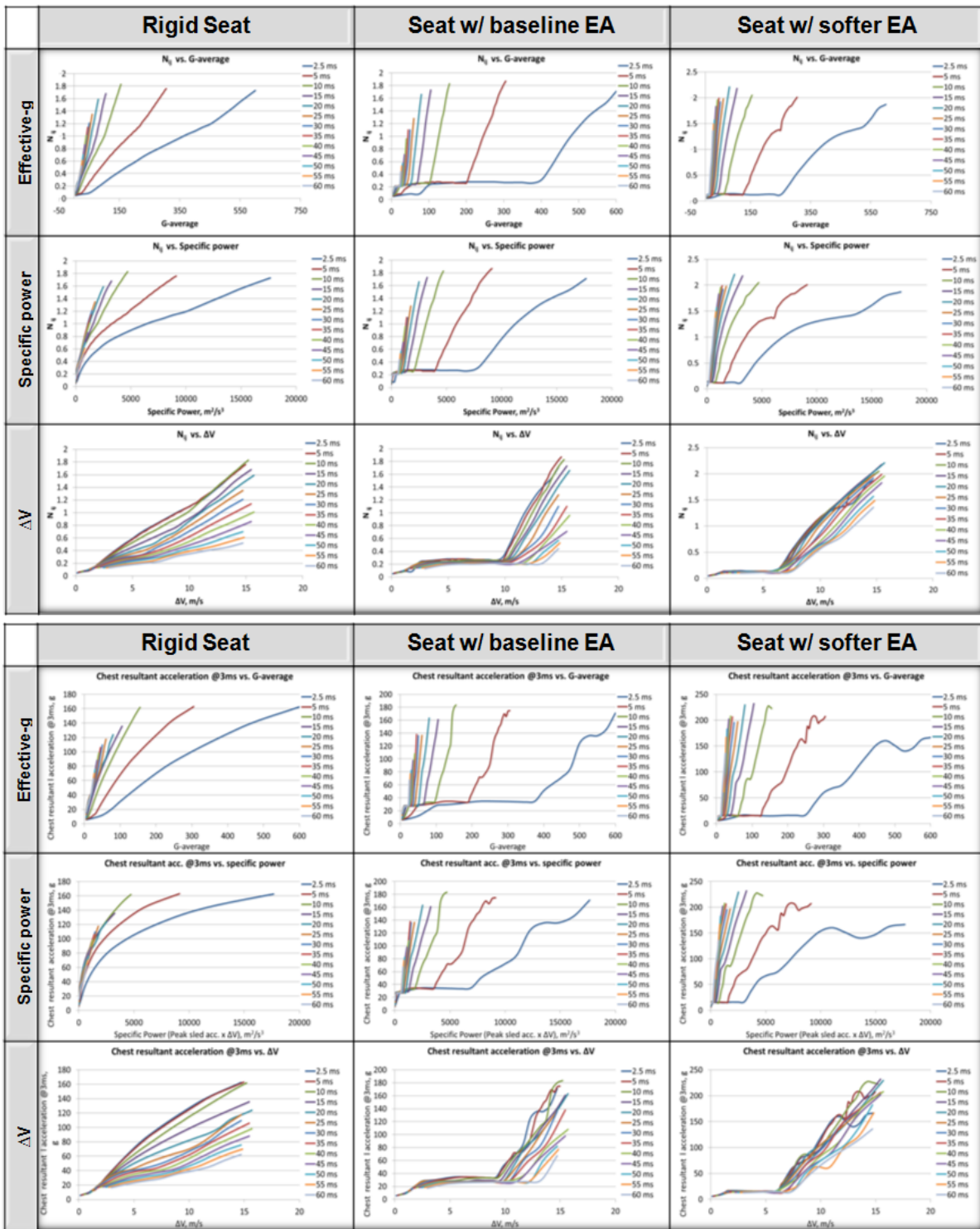
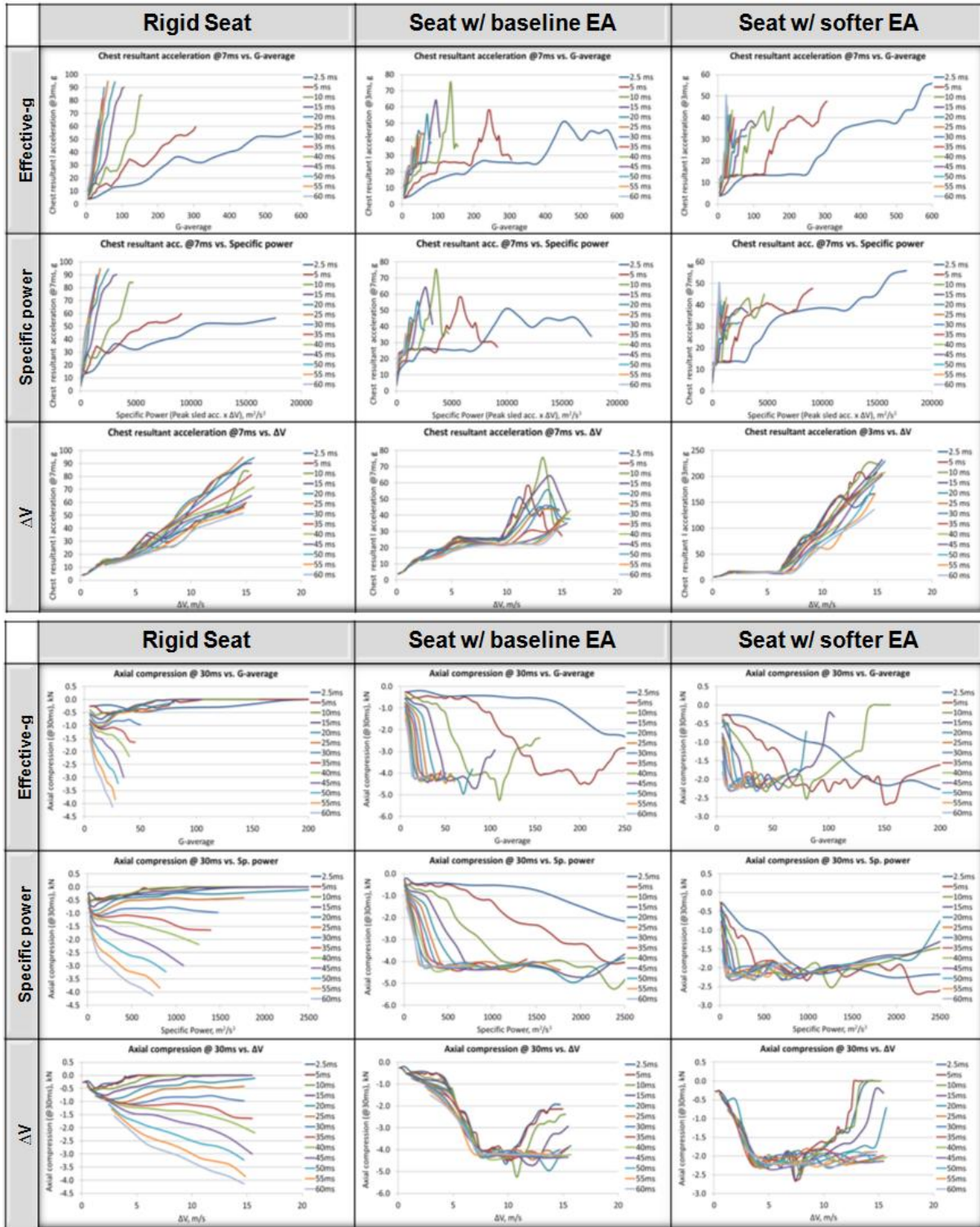


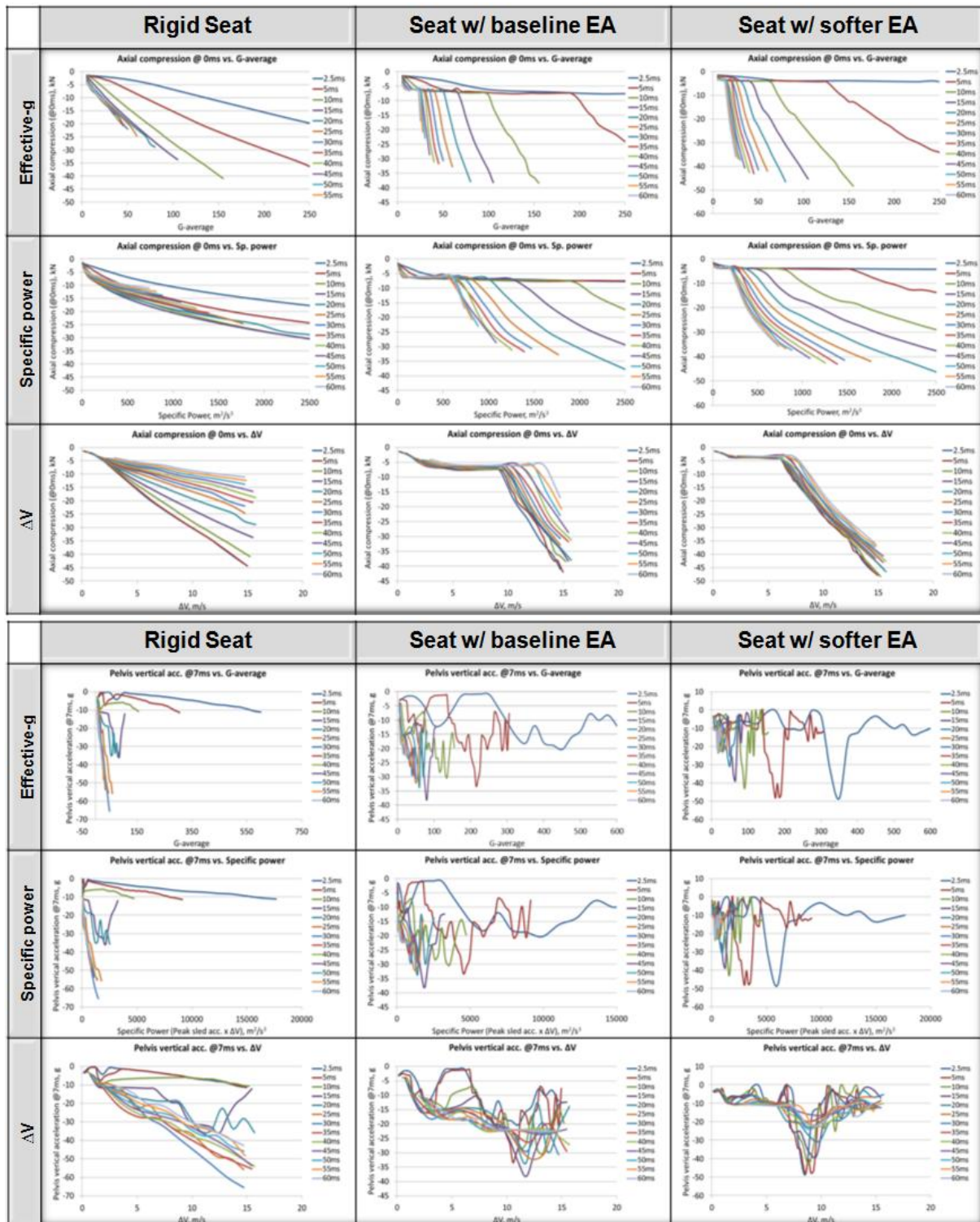
**Table A10-5, A10-6:** Chest resultant acceleration 7ms clip (Top) and Lumbar compression 30ms clip (Bottom) vs. blast loading parameters for three different seat types



Evaluating the Effectiveness of Various Blast Loading Descriptors as Occupant Injury Predictors... Kulkarni et. al  
 UNCLASSIFIED: Distribution Statement A. Approved for public release.



**Table A10-7, A10-8:** Peak lumbar compression (Top) and Pelvis vertical acceleration 7ms clip (Bottom) vs. blast loading parameters for three different seat types



Evaluating the Effectiveness of Various Blast Loading Descriptors as Occupant Injury Predictors... Kulkarni et. al  
 UNCLASSIFIED: Distribution Statement A. Approved for public release.